Jb. Geol. B.-A.	ISSN 0016-7800	Band **131**	Heft 4	S. 533–551	Wien, Dezember 1988

Post-Collisional Magmatism in the Ortler-Cevedale Massif (Northern Italy)

By GIORGIO V. DAL PIAZ, ALDO DEL MORO, SILVANA MARTIN & GIAMPIERO VENTURELLI*)

With 9 Figures and 4 Tables

Italy
Eastern Alps
Post-collisional magmatism
Oligocene
Mineral composition
Geochemistry
Geochronology

Contents

Zusammenfassung

Im Zuge der magmatischen Ereignisse, die sich nach der Kollision der Kontintente entlang der Periadriatischen Zone abspielten, intrudierten im Oligozän (32–31 Ma) an der Südseite des Ortler-Cevedale-Massivs der Rhätischen Alpen einige quarzdioritische Plutone und andesitische Gänge. Diese Körper drangen nach der Deckenüberschiebung in die Sedimenthülle und die kristalline Unterlage der oberostalpinen Ortler-Decke ein und erzeugten einen großen thermometamorphen Hof.

Zwei Gruppen magmatischer Körper mit kalkalkalischer und kalireicher kalkalkalisch/shoshonitischer Affinität sind in zwei benachbarten, voneinander getrennten Räumen erkannt worden. Die kalkalkalische Gruppe erfaßt den Quarzdioritpluton der Königsspitze und die andesitischen Gänge des Forno-Tales. Kalziumreiche Plagioklase, braungrüne Amphibole, etwas Biotit und Quarz bilden den Hauptmineralbestand; Kalifeldspat, Orthopyroxen, Klinopyroxen und Granat sind charakteristische akzessorische Minerale.

Die kalireiche Gruppe ist durch die Intrusiva vom Ulten-Tal und vom Mare-Tal (Peio) und durch die andesitischen Gänge des Gavia-Tales vertreten, welche hauptsächlich aus kalziumreichem Plagioklas, Amphibol, Biotit, Kalifeldspat und Quarz bestehen und ±Klinopyroxen aufweisen. Diese Gesteine unterscheiden sich nach ihrem Chemismus und nach ihrem Isotopengehalt, sodaß man annehmen kann, daß sie mindestens zwei verschiedenen Magmen des Mantels entstammen. Eine durch vielphasigen Prozeß verursachte, komplexe Entwicklung ist für die Entstehung der oligozänen magmatischen Tätigkeit ins Auge zu fassen:

1) Metasomatische Vorgänge haben während der frühalpidischen, kretazischen Subduktion jene Mantelteile verändert, welche später die Bezugsquellen der periadriatischen Magmen darstellten.
2) Diese Bezugsquellen wurden nach der Kollision der Kontinente dann aktiv, als im Eozän die geeigneten Wärmebedingungen wiederhergestellt waren.
3) Das Aufdringen der Magmen erfolgte, während im Oligozän auf kurze Zeit entlang der Periadritischen Zone Dehnungsbedingungen bestanden; durch die jungalpidische neogene Kompression wurde es am Aufdringen gehindert.

Die Kristallisationsdifferentiation der Muttermagmen gibt neben der wechselnden Einwirkung des Krustenmaterials eine weitere Erklärung für die Entstehung, den Chemismus und den Isotopengehalt dieser Gesteine.

Abstract

During the post collisional magmatic event which developed along the Periadriatic belt, some quartzdioritic plutons and

*) Authors' addresses: GIORGIO V. DAL PIAZ, SILVANA MARTIN, Istituto di Geologia dell' Università, via Giotto 1, I-35100 Padova; ALDO DEL MORO, Istituto di Geocronologia e Geochimica Isotopica CNR, via Cardinale Maffi 36, I-56100 Pisa; GIAMPIERO VENTURELLI, Istituto di Petrografia dell'Università, viale delle Scienze 78, I-43100 Parma.
Financial support for this study was provided by the "Centro di studio sull'Orogeno delle Alpi orientali", CNR Padova, and by the Ministero della Pubblica Istruzione.

andesitic dykes were emplaced (32–31 Ma ago) in the southeastern side of the Ortler-Cevedale Massif, Italian Rhaetian Alps. These bodies cut the cover and basement rocks of the Upper Austroalpine Ortler nappe after nappe piling and related shear zones, Eo-Alpine metamorphism and post nappe folding, and produced large thermometamorphic aureoles.

Two groups of magmatic bodies with calc-alkaline and high-K calc-alkaline/shoshonitic affinity have been recognized in two adjacent and separate areas. The calc-alkaline group includes the Gran Zebrù quartzdioritic pluton and the Forno valley andesitic dykes. Calcic plagioclase, brown-green amphibole, minor biotite and quartz are the main magmatic minerals, while K-feldspar, orthopyroxene, clinopyroxene and garnet sometimes occur as significant accessory minerals. The high-K calc-alkaline/shoshonitic group is represented by the Grünsee and Mare valley intrusive complexes and by the Gavia valley dykes, which are mainly formed of calcic plagioclase, amphibole, biotite, K-feldspar, quartz and ± clinopyroxene. The rocks studied display chemical and isotopic heterogeneities which suggest that the magmatic bodies of the Ortler-Cevedale massif were generated from at least two different mantle-derived parental magmas produced by different sources. A complex evolution by multistage processes for the genesis of the Oligocene magmatic activity may be envisaged as follows:

1) Metasomatic processes during the Eo-Alpine (Cretaceous) subduction allowed heterogeneities in the mantle sections which later acted as undercrustal sources of magmas.
2) These sources became active after the continental collision, when suitable thermal conditions were restored (Eocene).
3) The uprise of magmas occurred when extensional conditions briefly acted along the Periadriatic belt (Late Oligocene), and was averted by the renewal of Neo-Alpine compressive to transpressive regimes (Neogene).

Fractional processes of parental magmas in crustal magmatic chambers, combined with interaction with continental material, may further account for the genesis of these rocks and for their chemical and isotopic variations.

Riassunto

I plutoni quarzodioritici ed i filoni andesitici presenti nel settore sudorientale del massiccio dell'Ortles-Cevedale risalgono all'Oligocene superiore (32–31 Ma) ed appartengono quindi all'evento magmatico Periadriatico che si è sviluppato, lungo il settore interno della catena alpina, dopo la collisione continentale. Essi sono intrusi nelle coperture mesozoiche e nel basamento della falda dell'Ortles (Austroalpino superiore) e, in base a rapporti di intersezione, sono chiaramente successivi all'appilamento delle falde, allo sviluppo di zone di shear e di retrocessione metamorfica di età eoalpina e ad una fase di ripiegamento.

Lo studio geochimico ed isotopico consente di riconoscere due gruppi di rocce eruttive caratterizzati da affinità calcalcalina e calcalcalina alta in K/shoshonitica, localizzati in due aree separate ed adiacenti. Il primo gruppo comprende il plutone del Gran Zebrù ed i filoni della valle dei Forni e delle sue tributarie. La loro associazione magmatica è caratterizzata da plagioclasio calcico, anfibolo verde-bruno, biotite e quarzo cui talora si aggiungono, in quantità accessoria, feldspato potassico, pirosseni e granato. Il secondo gruppo comprende i complessi intrusivi del Lago Verde (valle d'Ultimo) e di valle della Mare (Peio) ed i filoni andesitici della valle del Gavia. I componenti fondamentali dell'associazione magmatica sono analoghi a quelli sopra descritti, integrati da feldspato potassico.

Il quadro dei caratteri geochimici ed isotopici suggerisce che i corpi eruttivi del massiccio dell'Ortles-Cevedale sono stati generati da almeno due magmi distinti, di derivazione sottocrostale. La loro genesi sembra legata a complessi processi polistadiali sintetizzabili nel modo sequente:

1) Processi metasomatici sviluppati nella zona di subduzione eoalpina hanno variamente anomalizzato parte delle sezioni di mantello che successivamente costituiranno le sorgenti dei magmi Periadriatici.
2) Tali sorgenti divennero attive soltanto con la normalizzazione dell'assetto termico della zona di collisione litosferica (Eocene).
3) La risalita dei magmi ebbe infine luogo quando la fascia Periadriatica fu sottoposta a vigorose condizioni distensive (Oligocene superiore) e l'attività magmatica cessò con il sopravvenire di nuovi regimi compressivi e transpressivi (Neogene).

Processi di frazionamento dei magmi parentali insediati in camere magmatiche crostali ed una certa interazione con materiale crostale completano il quadro dei processi evolutivi che hanno caratterizzato il magmatismo oligocenico in questa regione.

1. Introduction

The post collisional evolution of the Alps is characterized more or less continually by compressional conditions, mainly recorded by the Mesoalpine (or Lepontine) tectono-metamorphic event and by the Neoalpine deformational phases yielding Eocene–Lower Oligocene and Neogene ages respectively (TRÜMPY, 1973; LAUBSCHER & BERNOULLI, 1982; HUNZIKER & MARTINOTTI, 1987).

The post collisional evolution is also characterized by noticeable magmatic activity, displaying a calc-alkaline to ultrapotassic affinity (BECCALUVA et al., 1979, 1985; DAL PIAZ et al., 1979; BELLIENI et al., 1981; VENTURELLI et al., 1984; CALLEGARI, 1985, and references therein). It developed along the central-internal sector of the Alpine chain, mostly during the Late Oligocene, as recorded by the E–W-trending magmatic belt which, from the lower Aosta valley to Maribor, approximately follows the Periadriatic (or Insubric s.l.) fault system (Fig. 1) (GANSSER, 1968; BOEGHEL, 1975; EXNER, 1976; DAL PIAZ & VENTURELLI, 1985; LAUBSCHER, 1985, and references therein). This event is usually known as the Periadriatic magmatism, although it occurred far from the Adriatic Sea and earlier than the present structural setting of the Periadriatic Lineament was acquired (mainly Late Miocene, LAUBSCHER, 1985).

The Periadriatic magmatism generated plutons, stocks, thin elongated bodies (i.e. the lamellae of the Austrian literature), numerous dykes and poorly preserved volcanic and volcanoclastic covers (EXNER, 1976; DAL PIAZ [Ed.] 1985, and references therein). Most of these are located along and north of the Periadriatic fault system and intruded into the continent/continent collision suture of the Europe-verging Alpine pile of nappes, shortly after the Mesoalpine re-

Fig. 1.
Tectonic map of the Alps and location of Tertiary magmatic bodies along the Periadriatic belt. Dotted insert refers to Figs. 2 and 5.
1 = Austroalpine décollement nappes of Northern Calcareous Alps (NCA); 2 = Austroalpine basement and cover units (A); 3 = Pennine nappe system (P), including undifferentiated flysch and ophiolite units; 4 = Helvetic-Dauphinois décollement nappes an sedimentary covers (H); 5 = Helvetic-Dauphinois basement units; 6 = Southern Alps (SA); 7 = Dinarides (D); 8 = Oligocene and Neogene sedimentary basins (a = Bresse – Rhine graben system, Molasse foredeep, Piedmont – Langhe and Gonfolite basins, eastern Alpine intramontane basins; b = Vienna, Graz and Pannonian basins); 9 and 10 = Periadriatic magmatic bodies, mostly late Oligocene (9 = intrusive bodies; 10a = dykes; 10b = flows, tuffs and volcanoclastic covers).
Location of main plutons: 1 = Traversella; 2 = Biella; 3 = Novate; 4 = Bergell; 5 = Adamello; 6 = Gran Zebrù, Mare valley and Grünsee (this paper); 7 = Rumo and Samoclevo lamellae; 8 = northern portion of Bressanone body; 9 = Rensen and Mt. Alto; 10 = Cima di Vila; 11 = Vedrette di Ries (Rieserferner); 12–15 = lamellae and apophyses along eastern Periadriatic lines; 16 = Karawanken; 17 = Pohorje.

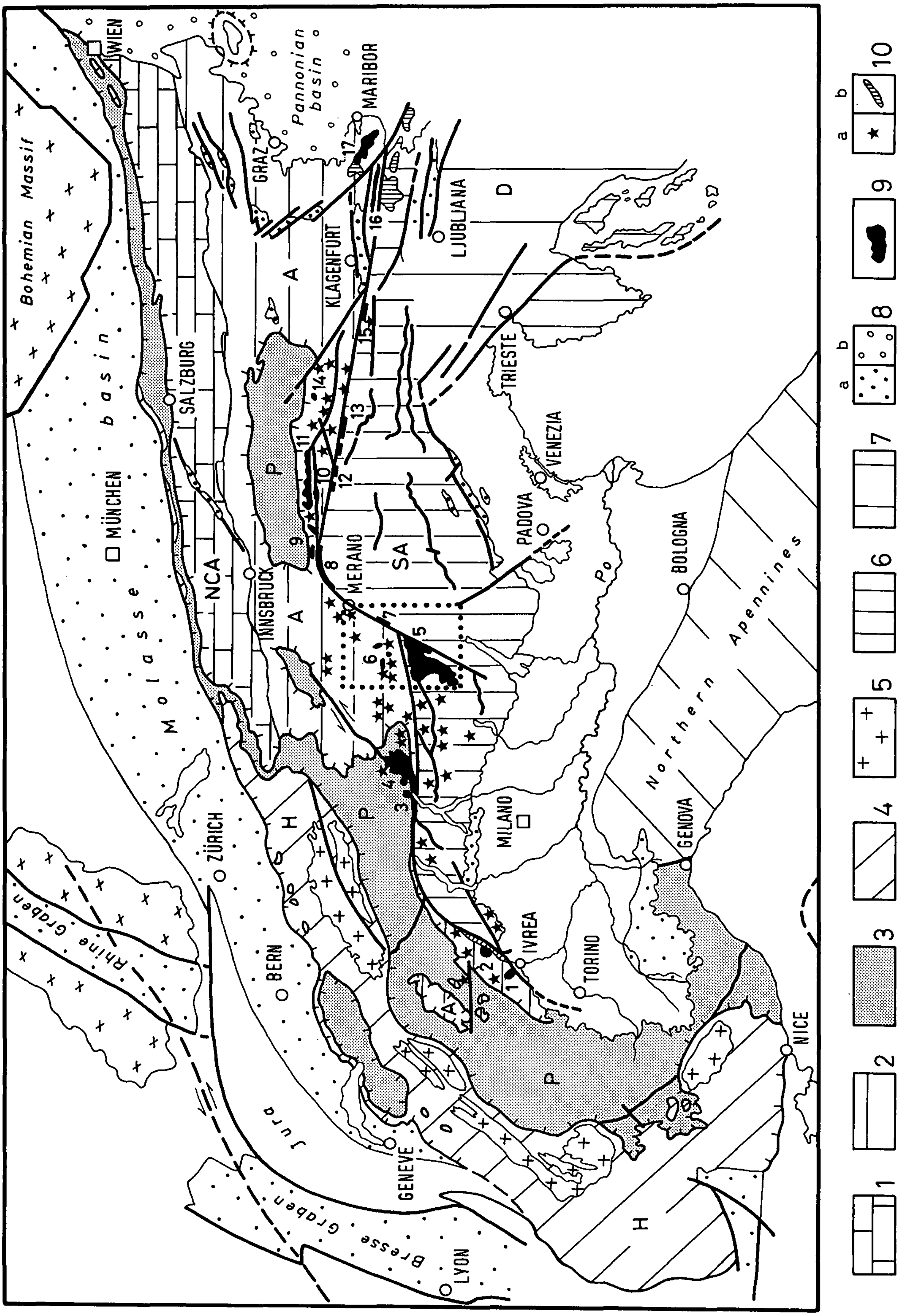
WIEN
Pannonian basin
MARIBOR
GRAZ
Bohemian Massif
SALZBURG
KLAGENFURT
LJUBLJANA
D
A
NCA
MÜNCHEN
Molasse basin
INNSBRUCK
MERANO
SA
P
TRIESTE
VENEZIA
PADOVA
Po
BOLOGNA
Northern Apennines
ZÜRICH
H
MILANO
GENOVA
IVREA
TORINO
BERN
Rhine Graben
Jura
GENEVE
NICE
Bresse Graben
LYON
1
2
3
4
5
6
7
8
9
10
11
12
13
14
15
16
17
a
b

gional metamorphism (DAL PIAZ et al., 1972, 1979); TROMMSDORFF & NIEVERGELT, 1985, and references therein). Others, including the Adamello composite batholith, were emplaced within the Africa-verging Southern Alps which, instead, seems to have excaped Mesoalpine effects (BRACK, 1981; CALLEGARI, 1985).

Except for some andesitic dykes, the timing of the Periadriatic magmatism is generally well defined by field interference patterns and numerous radiometric data (reviews in DAL PIAZ & LOMBARDO, 1985 and SASSI et al., 1985). Magmatic activity first appeared 42–35 Ma ago in the Southern Alps, south of the Mesoalpine chain, forming the southern and central Adamello plutons (DEL MORO et al., 1985) which include a former tholeiitic event (ULMER et al., 1985). Most of the magmas were emplaced along the Periadriatic Lineament and extensively northwards, from 33 to 29 Ma ago (clustering around 30 Ma), assisted by extensional conditions and acting briefly between the Mesoalpine and Neoalpine events (DAL PIAZ, 1976; DAL PIAZ & VENTURELLI, 1985; LAUBSCHER, 1985). The last uprise of magma occurred 25–24 Ma ago, as recorded by the Novate granite (GULSON, 1973) and by some dykes emplaced in the Austroalpine units south of the Tauern window (DEUTSCH, 1984).

A complex evolution by multistage processes may be suggested for the Periadriatic magmatism (DAL PIAZ et al., 1979; VENTURELLI et al., 1984; CALLEGARI, 1985; ULMER et al., 1985; SCHREYER et al., 1987, and references therein). Eo-Alpine lithospheric subduction produced the structural setting and, in some instances, the metasomatic processes in the mantle sections which later acted as undercrustal sources of magmas. These sources became active when a suitable thermal environment was restored at depth. Such conditions were probably reached in the Eocene, as inferred from the restoration of a normal gradient characterizing the post-collisional Lepontine metamorphism (FREY et al., 1974) and from the coeval rising of the oldest Adamello magmas. The plentiful Late Oligocene melts were emplaced when extension acted along the Periadriatic strip and was averted by the Neoalpine renewal of compressional regimes. Fractionation processes of parental magmas, combined with interaction with continental crust at different structural levels, account for the observed varieties in lithology, chemical composition and isotopic features (CALLEGARI, 1985; DEL MORO et al., 1985, and references therein).

The location of the melt sources cannot be univocally defined by the present position of the Periadriatic bodies, owing to Neoalpine tectonics. Although most of the Neoalpine shortening may have been accomodated outside the uplifting Mesoalpine chain and its innerlands by the external zones of both opposite-verging Alpine and Southalpine underplating systems, according to LAUBSCHER's (1971, 1974) models, some right-lateral and dip-slip shifting of the Periadriatic bodies from the lithospheric mantle roots my be envisaged.

This paper deals with some calc-alkaline plutons and dykes intruding the Austroalpine basement and cover units in the south-eastern side of the Ortler-Cevedale massif in the Italian Rhaetian Alps (Fig. 1). This is seen as a typical area for the post-collisional magmatism, being approximately located at the baricentre of the magmatic belt and, together with the Adamello batholith, forming the largest transversal section of the Periadriatic strip.

2. Areal Geology

The area examined here is located on the western side of the Trentino – Alto Adige (South Tyrol) region, near the boundary with Lombardy, between the Venosta (Vinschgau), Ultimo (Ulten), Sole and Gavia valleys (Fig. 2). It is mapped in the 1 : 100.000 Mt. Cevedale sheet (ANDREATTA, 1951).

For the basic literature on the regional geology of the Ortler-Cevedale massif and surroundig areas, reference may mostly be made to Gb. DAL PIAZ (1934, 1936, 1942), ANDREATTA (1935, 1948, 1954), POZZI (1965), GREGNANIN & PICCIRILLO (1972, 1974), GATTO & SCOLARI (1974), SATIR (1975), HERZBERG et al. (1977), PIRKL (1980), THÖNI (1981, 1986, and references therein) and, for the Alpine plutons and dykes, to STACHE & JOHN (1876), HAMMER (1908), G. DAL PIAZ (1926), KLEBELSBERG (1935), MINGUZZI (1940), ANDREATTA (1942, 1954), TOMBA (1947), CORNELIUS (1949), TOMASI (1960), ZANETTIN LORENZONI (1964), BARGOSSI et al. (1981), CERONI (1982) and FERRETTI TORRICELLI (1982). The serial and petrologic characterization of a noticeable set of dykes occurring in the south-western South Tyrol was made by GATTO et al. (1976) and BECCALUVA et al. (1979, 1985).

The Upper Austroalpine system exposed between the Tonale line and the Venosta valley includes the overlying Tonale high-grade basement unit and the underlying Ortler nappe, divided by a large, south-dipping, middle-angle shear zone, commonly known as the Peio Line (ANDREATTA, 1948). Further mylonitic to diaphtoritic zones, sometimes including anhydrite-gypsum lenses (Madriccio Pass, upper Peder valley; ANDREATTA, 1951), occur discontinuously inside the basement of the Ortler nappe, which is a stack of north-verging units. By comparison with other Austroalpine mylonites and from available data on the Alpine overprint in western South Tyrol (radiometric ages around 90 Ma; THÖNI, 1981), the Ortler shear zones may be assigned to the Eo-Alpine event.

The capping Tonale unit consists of pre-Alpine high-grade paragneisses and minor marbles, metabasites and gneissic granites, the latter transposed parallel to the regional schistosity, characterized by large schlingen structures. It also includes some slices of preserved to serpentinized spinel ± garnet lherzolites with a tectono-metamorphic fabric. The pelitic and psammitic sequences record a polyphase regional metamorphism which yields Hercynian radiometric mineral ages (THÖNI, 1981) and is characterized by sillimanite-kyanite-staurolite-garnet associations. Similar rocks reappear to the north (outside the bounds of Fig. 2), forming the Schlinig Klippe which overlies the Scarl cover nappe. As a whole, the capping basement unit may be seen as an intermediate crust plus upper mantle slices drawn out from the deep Southalpine domain and obducted on top of the Austroalpine nappe stack.

The underlying Ortler nappe is formed of medium- to low-grade continental crust, consisting of prevailing quartz-phyllites, strongly retrogressed paraschists and minor staurolite-bearing micaschists,

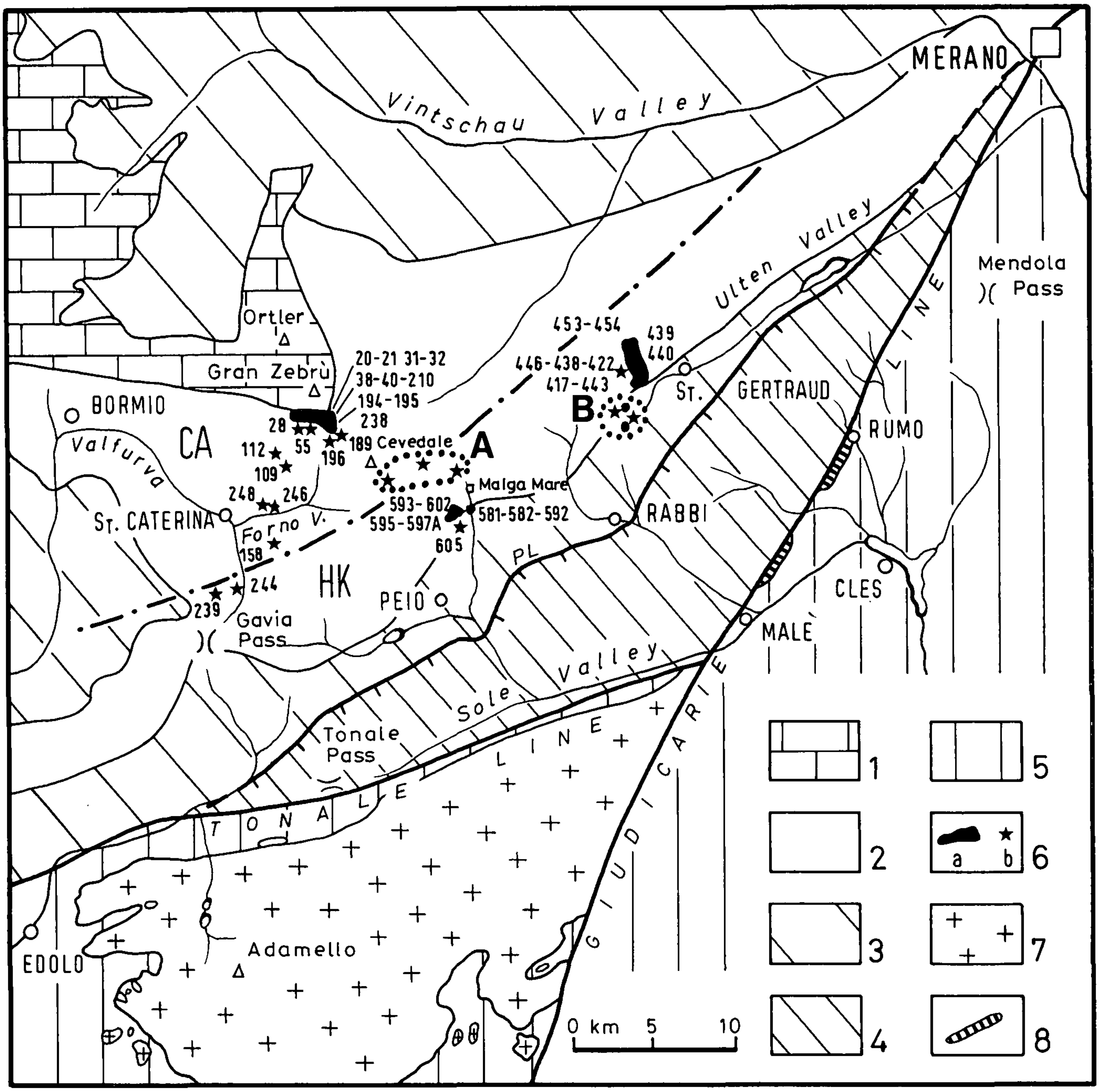

Fig. 2.
Sketch map of Austroalpine units, Southern Alps and Adamello batolith in Trentino-South Tyrol and Lombardy Regions and location of analysed magmatic bodies.
Upper Austroalpine system: 1 = sedimentary cover; 2 = quartz-phyllites and retrogressed paraschists; 3 = micaschists and paragneisses of Ortler nappe; 4 = high-grade paragneisses, orthogneisses, marbles, amphibolites and minor peridotites of Tonale unit.
Southern Alps: 5 = undifferentiated cover and basement sequences.
Analysed magmatic bodies: 6a = plutons, apohyses; 6b = dykes of calc-alkaline (CA) and high-K calc-alkaline/shoshonitic (HK) affinities (A and B = bodies studied by ANDREATTA, 1954, and MINGUZZI, 1940, respectively); 7 = Adamello batholith; 8 = Rumo and Somoclevo lamellae.
PL = Peio Line.

the latter preserved in the internal strip of the area. The quartz-phyllites in turn include beds of marbles and bodies of basic and acidic metavolcanics (ANDREATTA, 1954; ARGENTON et al., 1980; DAL PIAZ & MARTIN, 1980, and references therein). Most of the quartz phyllites, especially in the middle strip, are strongly retrogressed varieties of earlier medium-grade paraschists, which form an Eo-Alpine(?) steep shear belt extending from the upper Rumo valley to Lake Careser, Mt. Vioz and the Gavia pass.

Most of the sedimentary cover of the Upper Austroalpine basement is preserved westwards as stacks of décollement units, mainly consisting of recrystallized Triassic dolostones and limestones. The lowest unit, which is well exposed along the Ortler – Gran Zebrù (Königsspitze) ridge, may be interpreted as cover detached from the Ortler basement.

The Periadriatic magmatic bodies intruded both the Austroalpine units, the western side of the Peio Line, and the internal shear zones of the Ortler nappe. Plu-

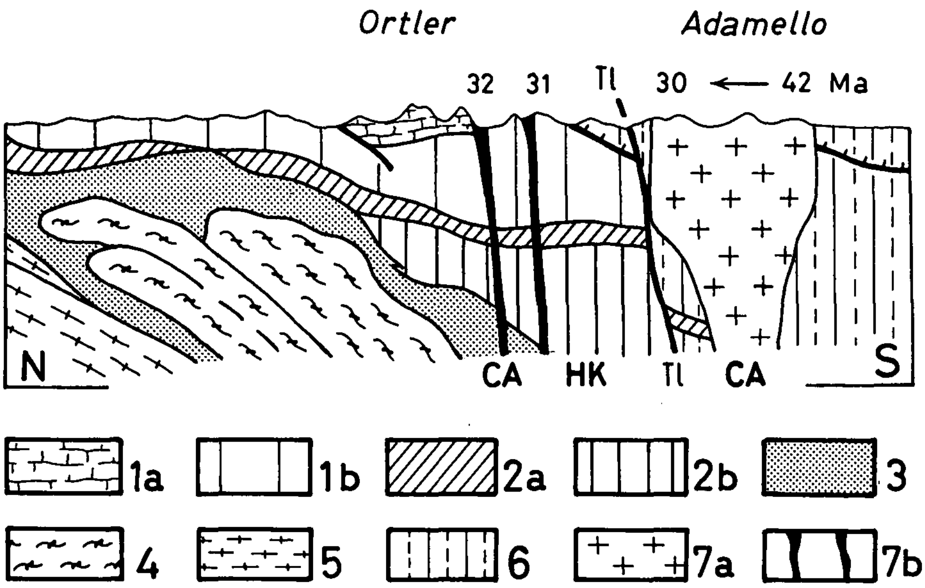

Fig. 3.
Tentative reconstruction of Alpine nappe pile along Adamello – Ortler section, and location of related Periadriatic bodies.
1 = Upper Austroalpine system: sedimentary cover (a) and basement units (b); 2 = Lower Austroalpine system: sedimentary cover (a) and basement units (b); 3 = Ophiolites, flysch décollement nappes and ocean-facing Paleoeuropean cover units; 4 = Penninic basement and cover units; 5 = Helvetic basement and cover units; 6 = Southalpine basement and cover units; 7 = post-collisional magmatic bodies: Adamello composite batholith (a), high-K calc-alkaline/shoshonitic (HK) Mare valley and calc-alkaline (CA) Gran Zebrù plutons (b).
TL = Tonale Line.

tons and dykes usually cut the regional schistosity and the parallel-transposed bedding.

The frame and composition of the units which, hidden in depth below the Ortler nappe, may have interacted with the Periadriatic magmas, are tentatively reconstructed in Fig. 3 by extrapolation from lateral sections of the nappe pile. From top to bottom, we expect to find:

1) The 10–15 km thick stack of Upper Austroalpine units;
2) the Lower Austroalpine system, consisting of upper continental basement with a clastic, volcanic and carbonate cover;
3) the ophiolitic suture, which may be correlated with the Malenco-Tauern sequences;
4) the internal belt of the gneissic Pennine ± Helvetic basement units, mainly derived from granitic protoliths.

The absence of lower continental crust in the deepest section may plausibly be expected, considering that the rock volumes involved here were dragged down from the thinned paleo-European passive margin.

3. Magmatic Bodies

The post-collisional magmatic bodies emplaced in the Ortler nappe north of the Peio Line are the following:

1) The plutons of Pale Rosse – Bottiglia pass (Gran Zebrù) and Grünsee (St. Gertraud, upper Ulten valley);
2) the Pala della Donzella – Tof di Malè and Malga Prabon stocks (Mare valley, Peio);
3) some andesitic dykes.

The locations and mineral assemblages of the analysed samples are shown in Fig 2 and in the appendix. Fig. 2 also shows the location of some bodies investigated by MINGUZZI (1940) and ANDREATTA (1954).

Different structural leves of intrusion are exposed. The Gran Zebrù pluton and related dykes intruded both the Hercynian quartz-phyllites and the Triassic cover. The magmatic bodies from Grünsee and Mare valley are emplaced at the boundary between partly preserved staurolite-garnet-bearing micaschists and strongly retrogressed paraschists. Further dykes mainly cut the greenschist basement.

Field evidence shows that magmatic activity postdated the Upper Triassic sedimentary cover, the Eo-Alpine recrystallization and ductile deformation of the cover and basement sequences, and the blastomylonitic shear zones. The magmatic bodies in turn record some brittle deformations which may be referred to the Neoalpine events. Oriented textures similar to those occurring extensively in the north-eastern sector of Adamello and in some elongated bodies along the Periadriatic fault system (EXNER, 1976; CALLEGARI, 1985, and references therein) have been found only locally in this area.

From the chemical data (see later), the magmatic rocks may be subdivided into two groups, displaying calc-alkaline to high-K calc-alkaline/shoshonitic affinity and forming two distinct NE-trending belts (CA and HK in Figs. 2 and 3), approximately parallel to the Peio Line.

3.1. Calc-Alkaline Group

This group includes the Gran Zebrù pluton and numerous dykes occurring in the Forno valley and in the Manzina, Pisella and Cedec tributaries.

The Gran Zebrù pluton is a 3 km long, E–W-trending elongated body discontinuously exposed in the glacier areas between the upper Zebrù valley and the Pale Rosse and Bottiglia passes, at the base of the southern wall of the Gran Zebrù itself (TOMASI, 1950; ANDREATTA, 1951; MARTIN, 1978; ARGENTON et al., 1980). Northwards the pluton intrudes the Norian folded carbonates and southwards the steep quartz-phyllites complex. It developed a noticeable thermal aureole characterized by pyroxene-garnet-amphibole-rich skarns (on impure or metasomatized carbonates) and andalusite-cordierite-spinel-corundum-plagioclase-biotite assemblages (on metapelites).

The Gran Zebrù pluton mainly consists of granular to porphyritic quartzdiorite, minor tonalite and leucocratic differentiates.

The main magmatic minerals are represented by prevailing plagioclase phenocrysts, often finely zoned (An_{80-20}) and sometimes including relics of a first generation of calcic plagioclase, and by zoned brown and/or green amphibole, minor biotite and quartz. Magnetite, apatite, zircon, clinopyroxene (mostly as relict inclusions in amphibole) are the most common accessories; K-feldspar and orthopyroxene rarely occur. Rounded to flattened cognate mafic nodules are scattered, displaying the same mineral assemblage of the host rock, but with a greater amount of mafic phases.

Most of the igneous rocks are weakly to partly altered: saussurite ± epidote ± white mica replace plagioclase, and chlorite ± epidote, carbonate, rutile and sphene the mafic minerals.

Some generations of dykes are associated with the pluton. The oldest are porphyritic and characterized by plagioclase phenocrysts, brown-green amphibole ± minor biotite ± clinopyroxene ± rare garnet (sample P-55). The dykes sometimes include irregularly shaped to small rounded fragments of the country rocks and rarely show a weak thermal overprint. The most recent dykes are aplitic and micropegmatitic, while hydrothermal veinlets cut both intrusive rocks and andesitic dykes.

The dykes of the Forno valley (Molinelli waterfall, Ciose stream, Manzina and Pisella valleys) are mostly greyish, medium- to coarse-grained andesites with weakly to pervasively altered phenocrysts of plagioclase (saussurite, epidote, zeolite, white mica), brown and green amphibole (chlorite ± biotite) ± biotite (chlorite, sphene) (ARGENTON, 1978; ARGENTON et al., 1980). A dark green, fine grained, basaltic–andesitic dyke (P-248) occurs at the Molinelli waterfall, parallel to a thick andesitic dyke (P-246). It displays small phenocrysts of altered plagioclase, green amphibole and minor clinopyroxene.

3.2. High-K Calc-Alkaline/Shoshonitic Group

This group includes some intrusive apophyses located in the Mare valley north of Peio, the Grünsee pluton, related dykes and a 2 km long andesitic dyke running from the middle Gavia valley to the Alpe valley, far from the intrusive bodies. Surrounding rocks are represented by strongly retrogressed staurolite-garnet-bearing micaschists and/or quartz-phyllites.

In the Mare valley the intrusive rocks occur as three small bodies:

1) A 0,6 km² stock esposed along the south-eastern slope of the Pala della Donzella – Tof di Malè ridge, approximately mapped on the Mt. Cevedale sheet;
2) a small heterogeneous apophysis, crowded by mafic cognate nodules and xenoliths; it is located along the Cogolo – Malga Mare road 100 m north of Malga Prabon, and was named the Malga Prabon body by ANDREATTA (1954);
3) a smaller (40 m wide) recently discovered apophysis (CERONI, 1982; FERRETTI TORRICELLI, 1982) located near Silvestrè along the Malga Mare – Vallenaia track, 600 m east of the Tof di Malè body.

The contact with the surrounding paraschists is sharp or irregularly defined by branching or lit par lit injections of leucocratic differentiates.

As inferred from a large thermometamorphic zone, the Mare valley intrusive complex represents the scattered top apophyses and related dykes of a larger E–W-trending buried pluton. The inner portion of the contact aureole is marked by K-feldspar-plagioclase-sillimanite-corundum-green spinel-andalusite-biotite-bearing hornfelses. The igneous rocks are mainly represented by granular to porphyritic quartzdiorites, with mafic to leucocratic differentiates. The main magmatic assemblage includes zoned plagioclase (An_{70-20}), amphibole (often poikylitic over first-generation plagioclase), biotite, clinopyroxene and quartz. Accessory minerals, alteration products and mineral characteristics are very similar to those in the Gran Zebrù pluton. The occurrence of interstitial K-feldspar as main or even subordinate component is a discriminatory feature of these rocks, which appear to be transitional towards the monzonitic suite.

The Grünsee pluton occurs as a 2.5 km long N–trending body discontinously exposed along the shoulders of the valley. The magmatic body is emplaced in retrogressed micaschists and quartz-phyllites and produced a large thermal aureole. According to MINGUZZI (1940) it is mainly formed of quartzdioritic types, characterized by prevailing zoned plagioclase, amphibole, biotite and minor quartz, and by mafic quartz-diorites. K-feldspar is always present, but in lesser amounts than in the Mare valley bodies. Common accessory minerals are: clinopyroxene, opaques, apatite and zircon. The igneous rocks are very well preserved, but in places saussurite, epidote, sericite, calcite, chlorite and sphene occasionally occur as

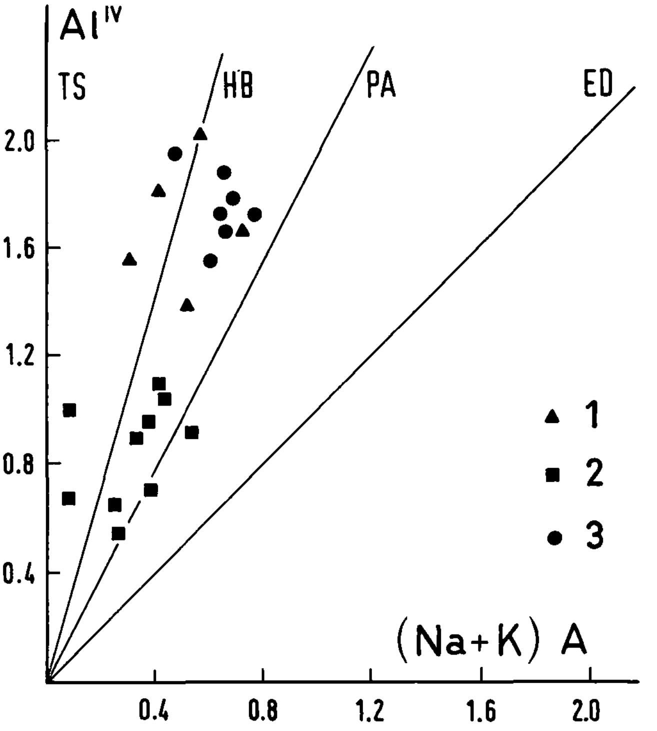

Fig. 4.
Al^{IV} vs (Na + K)A diagram showing composition of magmatic amphiboles from calc-alkaline rocks (1 = Molinelli waterfall dyke, D-248; 2 = Bottiglia pass quartzdiorite, P-31) and high-K calc-alkaline/shoshonitic rocks (3 = Gavia valley dyke, D-239).

minor alteration products. Cognate mafic nodules and xenoliths are common.

Some andesitic dykes occur in the surrounding paraschists. They display large phenocrysts of zoned plagioclase, amphibole and biotite, and include K-feldspar in the ground matrix. Aplite and fine-grained pegmatite dykes cut the plutonic rocks.

3.3. Mineral Composition

Microprobe analyses were carried out on the main magmatic minerals from the calc-alkaline basalt-andesite dykes (D-248, Molinelli waterfall, Forno valley) and the Gran Zebrù quartzdiorite (P-31, Bottiglia pass), and from one high-K calc-alkaline andesite dyke (P-239, middle Gavia valley). Some selected data on amphibole, pyroxene, biotite, plagioclase and K-feldspar are reported in Table 1.

The composition (IMA classification) of zoned phenocrystic amphibole from the Molinelli dyke ranges from alumino-tschermakite (brown core) to pargasite (green rim), while the small dark-green amphibole in the groundmass is represented by hastingsitic hornblende. The zoned phenocrysts from the Gavia valley dyke show quite similar evolution from pargasitic to hastingsitic composition. Pargasitic hornblende also represents the main mineral phase in some granular mafic concentrations included in the same dyke. The primary amphibole from the Bottiglia pass quartzdiorite displays Mg-hastingsite composition, and is partly replaced by a green actinolitic variety. Amphibole compositions are plotted in the Al^{IV} vs (Na + K)A diagram of Fig. 4.

Two texturally different clinopyroxenes occur in the Molinelli dyke, as colourless corroded phenocrysts and small grains growing round zoned amphibole phenocrysts. Their composition (diopside–salite) is similar to that of pyroxenes from the Mt. Mattoni and Mt. Blumone gabbros, southern Adamello (ULMER et al., 1985). The orthopyroxene from the quartzdiorite of the Bottiglia pass is a ferrosilite-term (Fs_{40-45}) with low (0–5) Wo content.

The composition of zoned plagioclase phenocrysts from dykes D-239 and D-248 ranges from bytownite to oligoclase. The K-feldspar occurring in the ground

Table 1.
Microprobe analyses of phenocrysts from calc-alkaline (CA) and high-K calc-alkaline/shoshonitic (HK) dykes (D) and plutonic rocks (P).

Samples	D-248 (CA)						P-31 (CA)				D-239 (HK)				
	Pl c	Pl r	Cpx		r Amph		Opx	Bi	Amph		Pl c	Pl r	KF	Amph c	Amph r
SiO_2	44.24	64.66	47.84	50.04	42.94	41.34	52.80	37.26	48.59	50.21	53.10	62.13	63.67	40.24	42.19
TiO_2	- -	- -	0.78	0.68	1.02	1.77	0.04	3.05	1.47	0.82	- -	0.04	0.22	1.55	1.56
Al_2O_3	34.71	22.23	5.39	4.97	9.52	13.98	- -	14.32	6.87	4.94	29.28	23.97	18.19	12.70	12.15
Cr_2O_3	- -	- -	- -	- -	- -	- -	0.21	- -	- -	- -	- -	- -	- -	- -	- -
FeO	0.75	0.23	8.76	7.68	20.90	11.78	25.00	20.90	14.54	16.07	0.45	0.15	0.28	19.34	14.88
MnO	- -	- -	0.20	0.06	0.88	0.12	1.28	0.52	0.49	0.77	- -	- -	- -	0.40	0.47
MgO	- -	- -	12.49	14.03	9.68	14.15	19.99	12.42	14.11	13.51	- -	- -	- -	8.52	12.17
CaO	18.77	2.43	23.91	22.05	11.62	12.40	0.88	- -	11.47	11.25	12.06	4.89	- -	11.11	11.84
Na_2O	1.39	10.16	- -	- -	0.45	1.23	- -	- -	- -	0.11	4.71	8.65	0.36	1.35	1.47
K_2O	0.02	0.10	- -	- -	0.96	1.20	- -	8.50	0.45	0.27	- -	0.14	16.33	1.96	1.19
Tot.	99.88	99.94	99.37	99.51	97.97	97.97	100.30	96.97	97.99	97.95	99.60	99.97	99.85	97.17	97.92
Si	8.218	11.391	1.797	1.863	6.439	5.992	1.998	5.602	7.028	7.316	9.653	11.008	11.819	6.191	6.244
Al^{IV}	7.601	4.617	0.203	0.137	1.561	2.008	- -	2.398	0.972	0.684	6.275	5.007	4.156	1.809	1.756
Al^{VI}	- -	- -	0.035	0.082	0.122	0.381	- -	0.142	0.199	0.165	- -	- -	- -	0.495	0.364
Ti	- -	- -	0.022	0.019	0.115	0.193	0.001	0.346	0.160	0.090	- -	0.005	0.046	0.179	0.174
Fe^{3+}	0.116	0.034	0.124	0.017	0.895	0.672	- -	- -	0.369	0.254	0.068	0.023	0.047	0.168	0.381
Cr	- -	- -	- -	- -	- -	- -	0.006	- -	- -	- -	- -	- -	- -	- -	- -
Fe^{2+}	- -	- -	0.151	0.222	1.726	0.756	0.790	2.629	1.390	1.704	- -	- -	- -	2.321	1.461
Mn	- -	- -	0.006	0.002	0.111	0.015	0.041	0.067	0.060	0.095	- -	- -	- -	0.052	0.059
Mg	- -	- -	0.699	0.779	2.163	3.057	1.125	2.784	3.042	2.934	--	--	--	1.953	2.684
Ca	3.736	0.459	0.962	0.880	1.867	1.926	0.036	- -	1.779	1.756	2.349	0.928	- -	1.831	1.877
Na	0.501	3.471	- -	- -	0.131	0.346	- -	- -	- -	0.033	1.660	2.972	0.130	0.403	0.437
K	0.005	0.022	- -	- -	0.184	0.222	- -	1.632	0.083	0.051	- -	0.032	3.868	0.385	0.226
Tot.	20.177	20.011	4.000	4.000	15.354	15.568	3.997	15.600	15.302	15.324	20.005	20.003	20.050	15.787	15.663

c: core; r: rim

Pl: plagioclase; Cpx: clinopyroxene; Amph: amphibole; Opx: orthopyroxene; Bi: biotite; KF: K-feldspar; The formulas for pyroxene and amphibole have been calculated according to PAPIKE et al.(1974); amphibole: O = 23; pyroxene: O = 6 and Σ cations = 4; feldspar: O = 32; biotite: O = 22. Sample location: D-248: Molinelli waterfall, Forno valley; P-31: Bottiglia Pass, Gran Zebrù; P-239: Gavia valley.

Table 2.
Rb-Sr analytical data on biotites.
(Analysts: U. GIANOTTI and G. PARDINI).

Sample		Locality	Rb ppm	Sr ppm	$^{87}Rb/^{86}Sr$	$(^{87}Sr/^{86}Sr)\pm1\sigma$	AGE$\pm1\sigma$ (Ma)
P 422	(Bi)	Grünsee (Ulten Valley)	472	13.6	101.0	0.7528± 9	31.4±0.8
P 454	(Bi)	Grünsee (Ulten Valley)	546	20.4	77.6	0.7415± 13	30.8±1.3
P 602	(Bi)	Tof di Malè (Peio Valley)	652	13.1	144.5	0.7709± 22	30.8±1.2
C 589	(Bi)	Prabon, (Peio Valley)	629	2.5	738.4	1.0501± 8	30.8±0.5
	(WR)		268	204.0	1.3	0.7286± 2	
P 32	(Bi)	Pale Rosse (Gran Zebrù)	350	4.7	215.1	0.8066± 10	32.4±0.6
P 40	(Bi)	Bottiglia Pass (Gran Zubrù)	312	7.7	117.3	0.7613± 6	32.1±0.6

Bi = biotite ; WR = whole rock; P = plutonic rocks; C = hornfels.

matrix of D-239 displays a low content of albite end-member.

4. Rb-Sr Radiometric Ages

Six determinations on the biotite-whole rock pair were carried out by the Rb-Sr method ($\lambda^{87}Rb = 1.42 \times 10^{-11}$/year). The analysed samples, from the Gran Zebrù, Mare valley and Grünsee plutons, are quartzdioritic types, with the exception of sample C-589, which is a biotite-clinopyroxene-amphibole-bearing hornfels produced by the Prabon apophyse (Mare valley) on the including paraschists. The obtained ages (Table 2) are in the range 32.4–30.8 Ma. A closely comparable age was found for the northern plutons of the Adamello composite batholith (DEL MORO et al., 1985), as mentioned above and sketched in Fig. 5.

5. Geochemistry and Sr Isotope Ratios

The analytical results obtained on 38 samples are reported in Tables 3 and 4. Analysed samples include 18

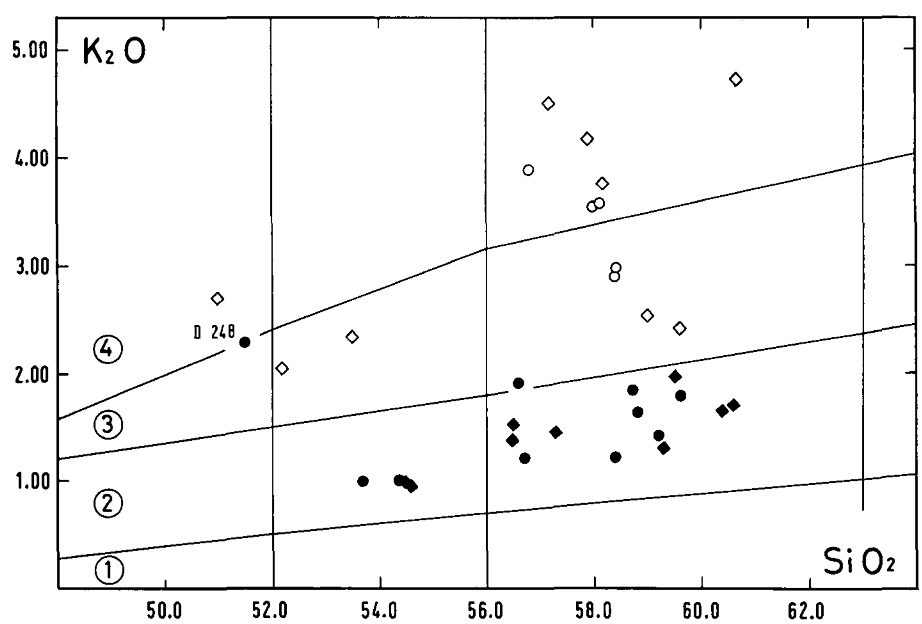

Fig. 6.
K_2O vs SiO_2 diagram for investigated rocks, divided into two main groups: calc-alkaline (CA; ● = dykes, ◆ = intrusive bodies) and high-K calc-alkaline/shoshonitic (HK; ○ = dykes, ◇ = intrusive bodies).
Mafic cognate nuclei and aplite-pegmatite dykes are not reported. Although characterized by high K_2O content, on the basis of trace elements sample D-248 (Molinelli waterfall) has been attributed to calc-alkaline group.
1 = Tholeiitic, 2 = calc-alkaline, 3 = high-K calc-alkaline and 4 = shoshonitic series.

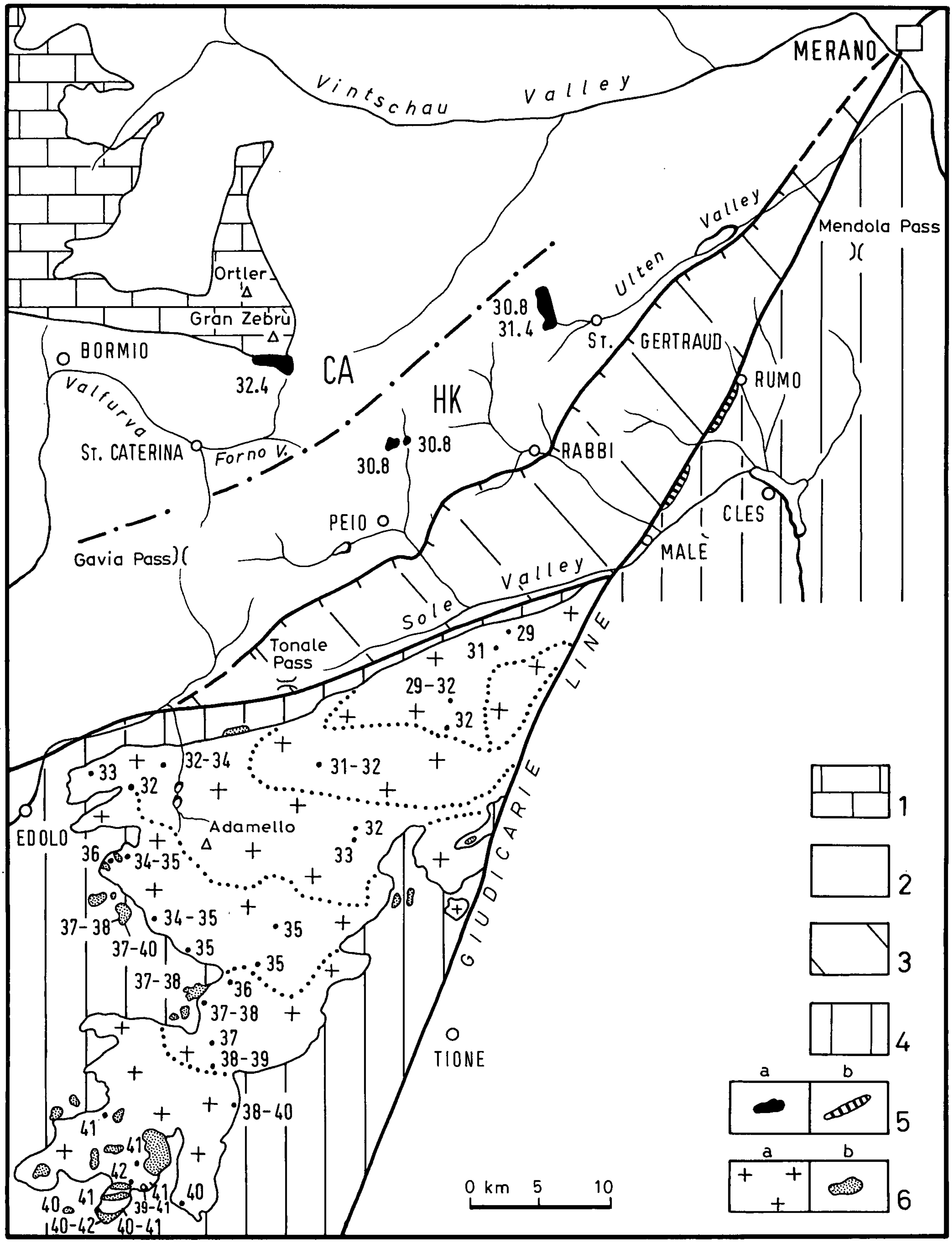

Fig. 5.
Distribution of radiometric ages (Ma) of plutons studied in this paper and of Adamello composite batholith (DEL MORO et al., 1985).
1 = sedimentary cover and 2 = basement rocks of the Ortler nappe; 3 = Tonale unit; 4 = Southern Alps; 5 = post-collisional magmatic bodies: a = Gran Zebrù, Mare valley and Grünsee plutons, b = Rumo and Samoclevo lamellae; 6 = Adamello batholith: a = granodiorite–tonalite plutons, b = gabbro bodies.

Table 3.
Chemical and isotopic (U. GIANNOTTI and G. PARDINI) data on calc-alkaline dykes (D) and intrusive rocks (P) from the NW sector of the investigated area (Forno valley and Gran Zebrù).

	FORNO VALLEY					GRAN ZEBRU'													
	D-248	D-112	D-246	D-158	D-109	D-189	D-55	D-196	D-28	D-238	P-194	P-195	P-32	P-21	P-31	P-40	P-210	P-20	P-38
SiO_2	51.50	56.60	56.70	58.80	59.20	54.40	58.40	59.60	58.70	53.70	54.50	54.60	56.50	56.50	57.30	59.30	59.50	60.40	60.60
TiO_2	.85	.60	.60	.50	.47	.73	.59	.49	.73	.72	.64	.54	.67	1.14	.61	.53	.49	.54	.47
Al_2O_3	17.40	18.00	17.30	18.00	18.50	18.50	18.20	18.20	18.10	18.40	18.80	20.90	18.00	16.60	17.80	17.40	17.10	17.80	18.20
Fe_2O_3	3.63	2.52	2.58	2.07	2.54	2.76	.59	2.73	1.38	2.97	2.90	2.89	1.98	1.08	2.20	2.28	.95	.96	1.27
FeO	5.13	4.36	4.04	3.55	2.82	5.01	5.10	2.81	5.05	5.05	4.51	3.80	5.17	5.32	4.65	3.54	4.37	4.14	3.54
MnO	.15	.17	.14	.14	.15	.16	.18	.07	.14	.17	.16	.14	.15	.14	.14	.11	.10	.11	.11
MgO	4.19	2.66	3.28	2.55	2.54	3.72	3.14	1.97	2.90	3.92	4.20	2.52	3.73	4.85	3.38	2.52	2.63	2.26	2.58
CaO	6.67	4.12	7.41	6.38	5.20	8.76	7.30	7.52	6.14	8.82	8.94	9.31	7.90	6.83	7.59	7.12	5.09	5.90	5.96
Na_2O	3.05	4.09	2.87	2.92	3.90	2.83	3.15	3.05	2.70	2.69	2.65	2.72	2.74	3.93	2.76	2.70	3.55	3.07	2.95
K_2O	2.28	1.90	1.21	1.64	1.41	.99	1.21	1.80	1.84	.98	.96	.92	1.38	1.50	1.43	1.30	1.97	1.63	1.69
P_2O_5	.24	.19	.12	.19	.13	.13	.13	.17	.16	.14	.14	.17	.13	.20	.13	.19	.13	.17	.14
L.O.I.	4.96	4.68	3.69	2.61	3.09	1.54	2.14	1.40	1.80	2.32	1.67	1.70	1.73	1.90	1.78	3.37	3.69	2.87	2.49
Total	100.05	99.89	99.94	99.35	99.95	99.53	100.13	99.81	99.64	99.88	100.07	100.21	100.08	99.99	99.77	100.36	99.57	99.85	100.00
Sc	34	20	26	20	17	31	25	15	29	37	32	19	34	24	31	29	21	13	20
V	260	133	171	110	109	234	141	89		353	189	149	186	141	166	135	131	96	
Cr	46	41	48	48	50	84	92	72		71	133	62	76	158	66	83	73	10	
Ni	16	5	11	10	9	16	15	11		17	131		13	42	11	14	10	5	
Rb	68	74	41	65	63	37	50	43 *	71	35	35	36	52	47	53	52	90	62	65
Sr	498	289	283	348	359	269	333	323 *	221	260	300	356	279	354	275	283	342	295	294
Th	6	12	6	9	(4)	(4)	6	6		(4)	(2)	(2)	(2)	7	(4)	(4)	7.5	8	
Zr	103	139	92	111	93	82	111	123	145	80	77	74	94	185	99	75	95	150	104
Nb	--	10	5	9	5.5	4	8	9	10	5	4	4	6	9	7	6	7	9	6
Y	24	27	20	21	19	20	22	24	29	26	24	17	24	32	23	21	17	26	12
Q	3.70	10.84	13.99	16.62	15.35	9.12	12.46	16.56	15.61	8.87	9.52	10.85	11.15	5.29	13.15	18.88	13.81	17.94	18.49
C	..	2.13	..	.23	1.38	..	..	..	.85	..	..	..	..	..	..	..	.15	.62	.98
Or	13.47	11.23	7.15	9.69	8.33	5.85	7.15	10.64	10.87	5.79	5.67	5.44	8.15	8.86	8.45	7.68	11.64	9.63	9.99
Ab	25.81	34.61	24.28	24.71	33.00	23.94	26.65	25.81	22.85	22.76	22.42	23.01	23.18	33.25	23.35	22.85	30.04	25.98	24.96
An	27.05	19.32	30.75	30.53	25.03	34.85	31.95	30.65	29.52	35.24	36.57	42.10	32.74	23.22	31.96	31.52	24.49	28.27	28.74
Di	3.75	..	4.31	..	..	6.40	2.90	4.56	..	6.27	5.63	2.51	4.66	7.72	4.03	2.19	..	..	..
Hy	13.92	11.87	10.63	10.59	8.91	12.15	14.62	4.93	14.41	12.65	12.86	9.01	14.03	15.57	12.41	9.15	13.17	11.75	11.30
Mt	5.26	3.65	3.74	3.00	3.68	4.00	.86	3.96	2.00	4.31	4.20	4.19	2.87	1.57	3.19	3.31	1.38	1.39	1.84
Il	1.61	1.14	1.14	.95	.89	1.39	1.12	.93	1.39	1.37	1.22	1.03	1.27	2.16	1.16	1.01	.93	1.03	.89
Ap	.52	.42	.26	.42	.28	.28	.28	.37	.35	.31	.31	.37	.28	.44	.28	.42	.28	.37	.31
D.I.	42.98	56.68	45.42	51.02	56.68	38.91	46.26	53.01	49.33	37.42	37.61	39.30	42.48	47.40	44.95	49.41	55.49	53.55	53.44
86/87 Sr	.7091±2	.7103±2	.7077±2	.7090±2	.7077±2	.7063±2	.7106±1	.7085±1	.7100±2	.7067±2	.7064±2	.7070±2	.7078±2	.7107±2	.7067±2	.7080±4	.7079±2	.7080±3	.7090±2
$(86/87\ Sr)_o$	.7089	.7100	.7075	.7088	.7075	.7061	.7104	.7083	.7096	.7065	.7063	.7069	.7076	.7105	.7064	.7078	.7077	.7077	.7087

o= initial ratio (31 Ma); ( )= less accurate data; Si,Ti,Al,Fetot,Mn,Ca,K,P,Sc,V,Ni,Cr,Zr,Y,Nb,Th have been determined by XRF, Na by phlame photometry, Mg by atomic absorption. Sr and Rb have been determined by XRF or by isotope dilution(*). All the isotopic analyses have been performed by a Varian Mat THS mass spectrometer. The Sr isotope composition has been normalized to 87/86 Sr for Eimer and Amend=0.70812±0.00008.

Table 4.
Chemical and isotopic data on high-K calc-alkaline/shoshonitic dykes (D), intrusive rocks (P), aplite/pegmatite dykes (A) and cognate mafic inclusions (M) from the SE sector of the investigated area.
For analytical methods and symbols see Table 3.

	GAVIA VALLEY		PALA DELLA DONZELLA-TOF DI MALE'-MALGA PRABON								GRUNSEE								
	D-239	D-244	D-605	P-582	P-602	P-597A	P-581	P-593	M-592	A-595	D-443	D-417	P-440	P-454	P-438	P-422	M-453	A-446	A-439
SiO_2	58.40	58.40	56.80	57.20	57.90	58.20	59.00	60.70	53.40	71.10	58.00	58.10	51.00	52.20	53.50	59.60	46.80	73.10	76.40
TiO_2	.58	.58	.72	.67	.68	.71	.69	.55	.83	.30	.74	.789	.86	.88	.83	.65	1.33	.20	.13
Al_2O_3	17.00	17.00	16.00	16.30	15.50	15.50	17.10	16.00	13.40	14.60	15.90	16.10	19.20	18.70	17.70	17.30	18.30	13.80	12.80
Fe_2O_3	1.99	1.96	2.11	2.34	1.25	5.16	1.36	1.96	1.59	.05	1.58	1.97	1.31	2.06	.77	.57	3.31	.14	.14
FeO	3.43	3.36	4.22	4.34	4.95	1.74	4.26	3.00	6.35	1.27	4.81	4.42	6.23	5.80	6.66	5.49	8.03	1.28	.27
MnO	.12	.12	.14	.15	.15	.13	.12	.10	.24	.03	.09	.10	.16	.16	.16	.13	.18	.03	.02
MgO	3.40	3.35	3.71	3.06	3.70	3.75	3.15	2.97	6.62	1.15	3.23	3.39	4.06	4.09	3.96	2.97	5.51	.47	.09
CaO	6.35	6.20	6.58	6.58	6.39	6.31	6.42	4.97	10.20	2.09	6.08	6.13	8.56	8.89	8.38	6.39	8.85	1.13	1.15
Na_2O	2.97	3.01	2.94	2.87	2.68	2.69	3.49	2.77	2.39	2.62	2.90	3.15	3.55	2.75	3.05	2.39	2.46	2.10	2.23
K_2O	2.90	2.96	3.88	4.49	4.16	3.74	2.53	4.71	2.46	5.08	3.54	3.56	2.69	2.04	2.33	2.41	2.42	6.56	6.16
P_2O_5	.33	.33	.53	.55	.50	.56	.55	.43	.43	.21	.44	.50	.60	.61	.60	.45	.71	.13	.03
L.O.I.	2.66	2.41	1.90	1.17	1.53	1.11	1.31	1.67	1.60	1.14	2.29	1.57	1.49	1.51	1.77	1.57	1.93	.77	.35
Total	100.13	99.68	99.53	99.72	99.39	99.60	99.98	99.83	99.51	99.64	99.60	99.78	99.71	99.69	99.71	99.92	99.83	99.71	99.77
Sc	25	22	24	20	23	23	21	20	41	10	22	20	24	24.5	25	19.5	30	5	3
V	150	157	178	182	170	172	186	133	208	54	173	175	218	240	217	171	366	18	20
Cr	83	60	72	39	76	79	39	66	181	26	40	42	46	33	34	30	25	14	7
Ni	21	20	14	11	20	17	16	14	31	17	13	15	20	14	14		20	10	6
Rb	130	143*	154*	176	187*	200	152	160	145	216	247	190	147	117*	109	147*	155	213	186
Sr	719	731*	812*	862	791*	711	819	776	577	379	837	998	974	835*	817	748*	797	400	328
Th	20	20	24	28	22	27	18	23	7	16	26	27	10	7	10	18	(2)		32
Zr	128	139	167	187	157	160	197	146	97	77	171	180	182	140	131	150	141	81	41
Nb	11	10	17	19	18	20	24	16	18	12	15	15	17	20	13	13	18	7	5
Y	22	20	26	25	22	25	31	22	23	19	21	25	30	34	32	24	32	15	6.5
Q	11.50	11.40	6.53	6.08	7.50	12.46	10.43	12.18	1.54	29.92	9.57	8.56	..	2.95	1.95	15.50	..	32.10	37.24
C	..	..	..	..	..	..	..	..	..	1.44	..	..	..	..	..	.11	..	1.47	.44
Or	17.14	17.49	22.93	26.53	24.58	22.10	14.95	27.83	14.54	30.02	20.92	21.04	15.90	12.05	13.77	14.24	14.30	38.76	36.40
Ab	25.13	25.47	24.88	24.28	22.68	22.76	29.53	23.44	20.22	22.17	24.54	26.65	28.38	23.27	25.81	20.22	20.81	17.77	18.87
An	24.49	24.13	19.00	18.33	17.98	19.17	23.52	17.31	18.57	9.13	19.91	19.28	28.51	32.66	27.72	29.05	31.74	4.84	5.53
Ne	..	..	..	..	..	..	..	..	..	..	..	..	.90	..	..	..	..	..	..
Di	4.10	3.78	8.54	9.05	8.85	6.88	4.17	3.88	23.98	..	6.29	6.68	8.60	6.45	8.56	..	6.54	..	..
Hy	10.41	10.33	10.17	8.40	12.08	6.15	11.58	8.69	14.25	4.71	11.42	10.55	..	14.81	16.13	16.17	1.93	3.13	.43
Ol	..	..	..	..	..	..	..	..	..	..	..	..	11.09	..	..	..	13.70	..	..
Mt	2.88	2.84	3.06	3.39	1.81	3.97	1.97	2.84	2.31	.07	2.29	2.86	1.90	2.99	1.12	.83	4.80	.20	.20
Il	1.10	1.10	1.37	1.27	1.29	1.35	1.31	1.04	1.58	.57	1.41	1.50	1.63	1.67	1.58	1.23	2.53	.38	.25
Hm	..	..	..	..	..	2.42	..	..	..	..	..	..	..	..	..	..	..	..	..
Ap	.72	.72	1.16	1.20	1.09	1.22	1.20	.94	.94	.46	.96	1.09	1.31	1.33	1.31	.98	1.55	.28	.07
D.I.	53.77	54.36	54.34	56.89	54.76	57.32	54.91	63.45	36.30	82.11	55.03	56.25	45.18	38.27	41.53	49.96	35.11	88.63	92.51
86/87 Sr	.7072±2	.7073±2	.7082±2		.7079±2						.7099±2	.7102±2		.7077±2		.7080±4			
$(86/87\ Sr)_o$	.7070	.7070	.7080		.7076						.7095	.7100		.7075		.7077			

plutonic rocks, 15 andesitic dykes, 3 aplite-pegmatite dykes and 2 cognate mafic nodules. Locations and mineral assemblages are summarized in the appendix (see also Fig. 2).

The plutonic rocks and dykes range in chemical composition from basalt-andesite to andesite (Fig. 6), but MgO is always low also in the less siliceous rocks. Only V, Sc, TiO_2 and SiO_2 correlate with magnesium. The correlation with Sc and V increases if only the dykes are considered. Zr, Nb, Th, Rb and K_2O (Fig. 7) show some correlation : in the Zr-Nb diagram only two samples (P-21 and P-454) fall far from the main trend. Rb and K_2O (Fig. 7) also correlate at low K_2O contents (less than 3 %), while at high K_2O values the data are scattered. The scatter may be partially due to the plutonic nature of the rock, which cannot always be regarded as representative of melts. The Rb and Sr concentrations cover a wide range (Rb: 35–247 ppm; Sr: 221–1167 ppm) while, excluding the aplite dykes, the range of the Rb/Sr ratio is rather narrow (0.10–0.32).

In the K_2O vs SiO_2 diagramm (Fig. 6) and according to the P_2O_5, Rb, Sr, Th, Zr, Sc and Mg contents, the analysed rocks are divided into two main groups (see, for instance, Fig. 8): calc-alkaline (CA) and high-K calc-alkaline/shoshonitic (HK), the latter being characterized by higher P_2O_5, K_2O, Rb, Sr, Th, Zr, Nb and TiO_2 and lower Sc. Both CA and HK families show a positive correlation between Rb and Rb/Sr ratios (Fig. 8) which is more evident in the calc-alkaline rocks.

The initial (31 Ma) $^{87}Sr/^{86}Sr$ ratio ranges from 0.7061 to 0.7105 (Tables 3 and 4). The calc-alkaline group displays a larger range (0.7061–0.7105) than the high-K calc-alkaline/shoshonitic group (0.7070–0.7100). Some samples with high $^{87}Sr/^{87}Sr$ ratio (e.g., dyke D-28 and plutonic rock P-21) contain quartz-phyllitic microxenoliths which constitute evidence of accidental crustal contamination during the last emplacement stages. Instead, variations in the initial strontium isotope ratio for the Gran Zebrù plutonic samples (P-210 and P-40 vs P-38) may be due either to different magmatic inputs

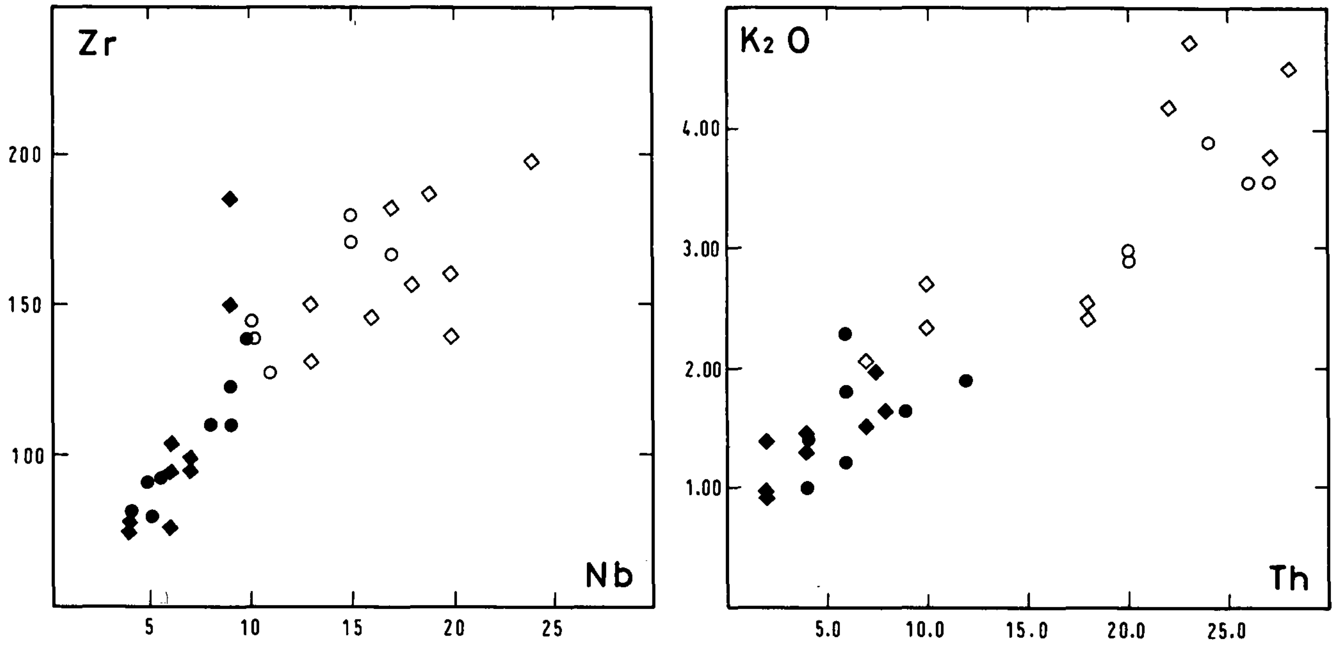

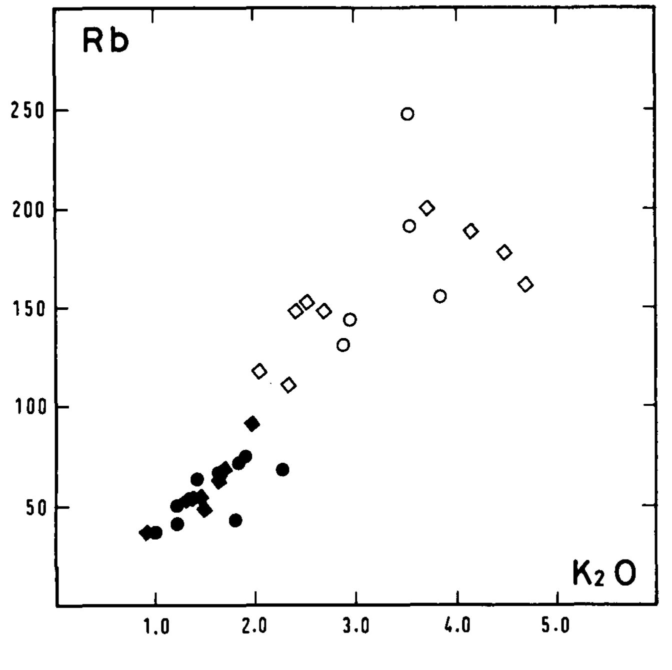

Fig. 7.
Zr – Nb, K_2O – Th and Rb – K_2O diagrams for investigated rocks.
Symbols as in Fig. 6.

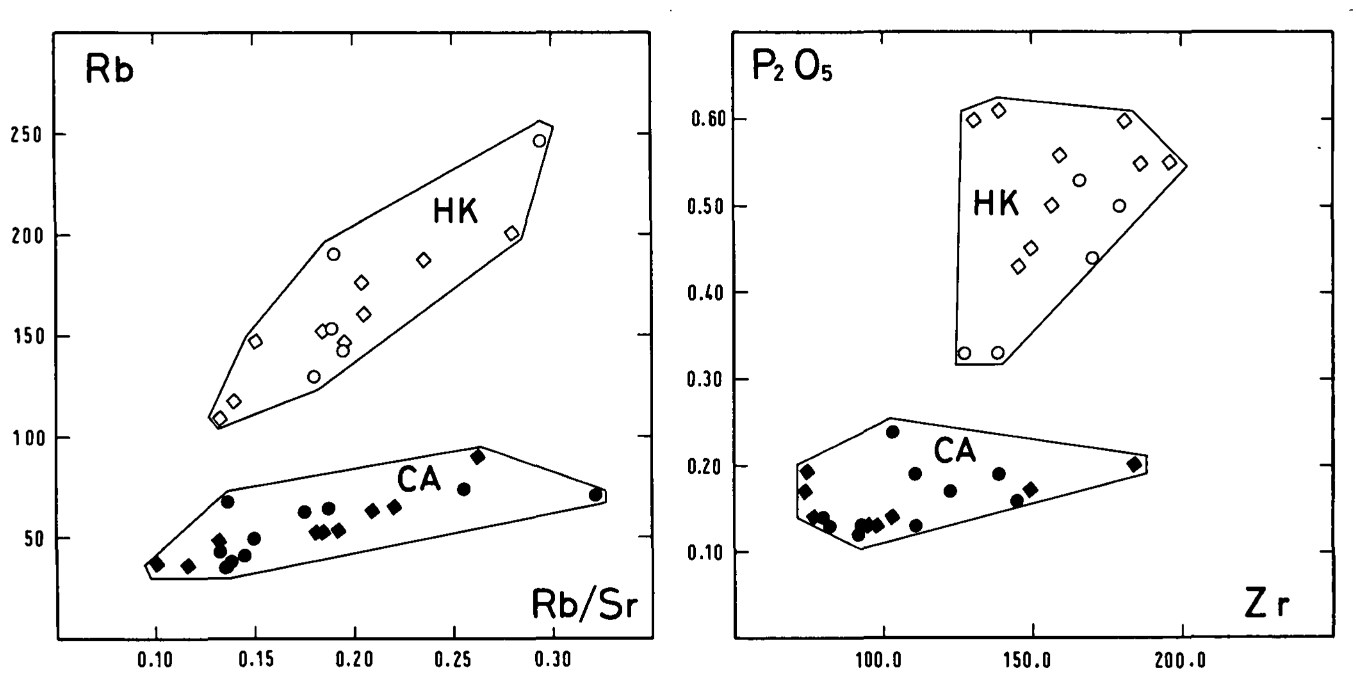

Fig. 8.
Rb – Rb/Sr and P_2O_5 – Zr diagrams for investigated rocks.
Calc-alkaline (CA) and high-K calc-alkaline/shoshonitic (HK) rocks fill different areas.
Symbols as in Fig. 6.

or to a variable degree of interaction between igneous rocks and deuteric fluids contaminated by crustal components.

The initial Sr isotope ratio is quite constant in other plutonic bodies (Grünsee, samples P-454, P-422: isotope ratio 0.7076±1; Cedec-Graglia ridge of Gran Zebrų intrusive complex, D-238, P-194, P-195: 0.7065±4) and in the large dyke of the Gavia valley (D-239, D-244: 0.7070).

6. Petrogenesis and Isotope Constraints

The investigated rocks show mineralogical, chemical and Sr isotopic features similar to those of the most frequent post-collisional magmatic products occurring along the Periadriatic belt. Moreover, in spite of their post-collisional origin, they are similar to the products generated at destructive continental margins by subduction of oceanic lithosphere.

As mentioned above, the studied rocks may be divided into two groups occurring in separate and adjacent areas (Fig. 2), where they were emplaced at 32–31 Ma (Fig. 5).

The positive correlations between Ni, V, Sc and MgO is compatible with the significant role played by fractional crystallization of ferro-magnesian minerals. However, the distribution of several elements in the CA and HK groups defines two different trends which cannot have been generated by fractional crystallization of a single magma but which require at least two parent magmas interacting with a crustal component. This large-scale heterogeneity of the magmas is also supported by the rough correlation between initial Sr ratio and some incompatible elements, e.g., $(^{87}Sr/^{86}Sr)_i$ vs Zr an Th (Fig. 9). The scatter within each rough trend in Fig. 9 may be due to:

1) further original small-scale heterogeneities;
2) interaction with fluids enriched in crustal components;
3) addition of small amounts of highly radiogenic country rocks.

If we assume that the melts are related to mantle derived parental magmas (Dal Piaz et al., 1979; Venturelli et al., 1984; Callegari, 1985; Del Moro et al., 1985; Kagami et al., 1985; Ulmer et al., 1985; Schreyer et al., 1987), the hypothesized source heterogeneities might result from interaction between mantle material and fluid melts released from the slab dragged down during Eo-Alpine subduction (Dal Piaz et al., 1979; Venturelli et al., 1984; Schreyer et al., 1987, and references therein), long before the magmatic sources became active.

7. Conclusions

1) The Tertiary magmatic activity with "orogenic" chemical features which characterized the whole east-west internal sector of the Alpine chain along the Periadriatic belt was related to multistage processes diachronously acting before and after continental collision:
   a) appropriate mantle sources were produced during the active subduction of oceanic lithosphere;
   b) partial melting of the source developed only when thermal restoration occurred;
   c) melt uprise and emplacement in crustal magmatic chambers took place when extensional tectonics operated (first in southern Adamello and then along the Periadriatic belt).
2) As for most sectors of the Periadriatic belt, magmatic activity in the investigated area developed 32–31 Ma ago.
3) Two different types of magmas (calc-alkaline and high-K calc-alkaline/shoshonitic) have been recognized; they were emplaced in adjacent and separated areas.

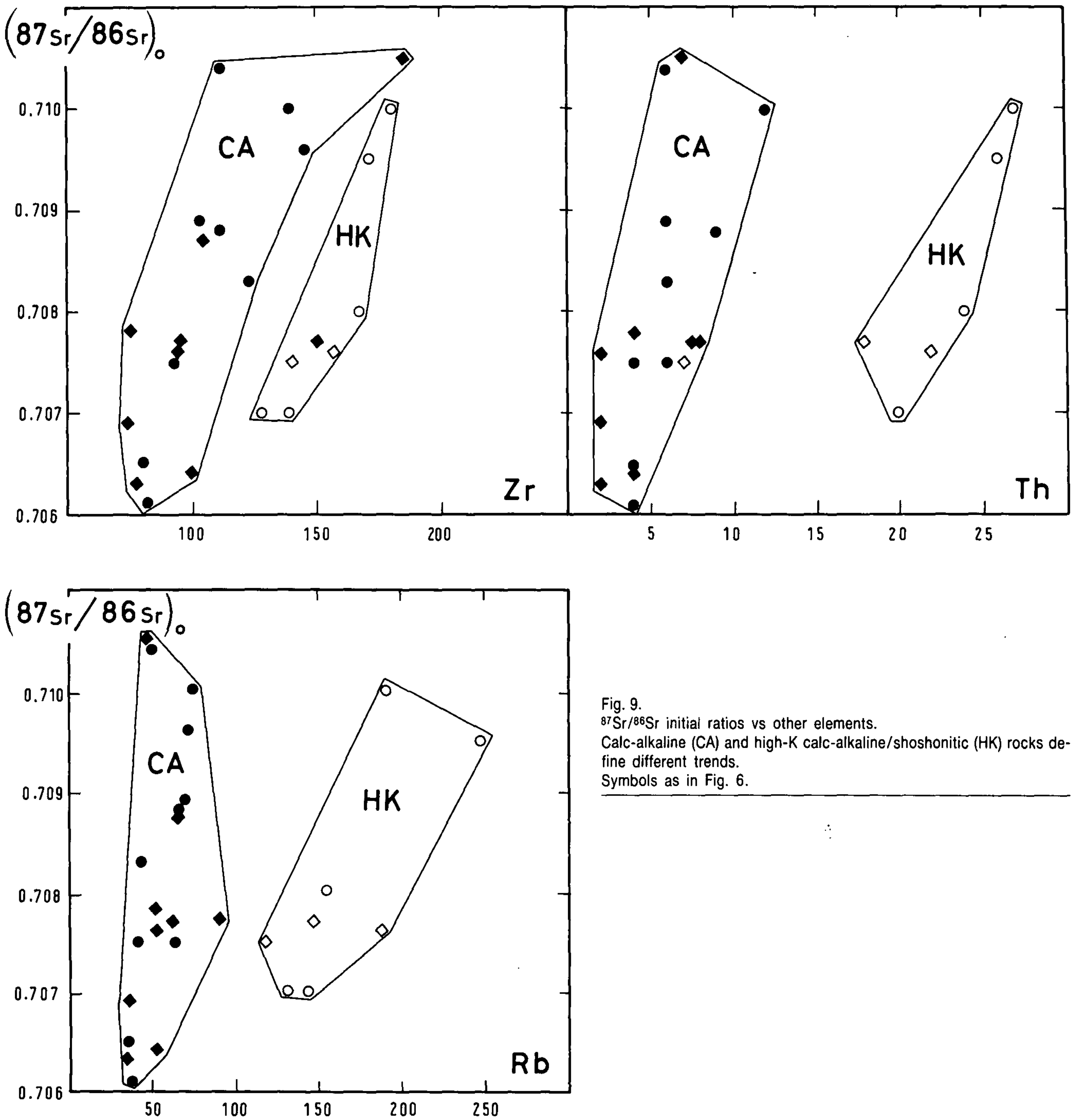

Fig. 9.
$^{87}Sr/^{86}Sr$ initial ratios vs other elements.
Calc-alkaline (CA) and high-K calc-alkaline/shoshonitic (HK) rocks define different trends.
Symbols as in Fig. 6.

4) The scatter of the Sr isotope data within the two magmatic series, besides to crustal microinclusions and assimilation, may be due to small-scale heterogeneities of the sources and to later interaction with deuteric fluids enriched in crustal components.

5) The chronology and distribution of the Oligocene magmatic products in the Ortler-Cevedale massif, as well as in the whole Periadriatic belt, do not fit the space and time vs composition relationship which characterizes most modern consuming plate margins.

Appendix

Mineralogical composition and location of the analysed samples.

SAMPLE	COMPOSITION	LOCATION
CALC-ALKALINE GROUP		
D-248	PL, HBL, CPX, qtz, op, ap, (chl), (ep), (cc)	Molinelli waterfall, Forno valley, 1952 m.
D-112	PL, HBL, qtz, bi, ap, op, zr, (chl), (ti), (ru), (cc), (wm), (ep)	High Pisella valley (northern side of the Forno valley), 3030 m, below Cime dei Forni.
D-246	PL, HBL, qtz, op, ap, (chl), (cc), (wm), (ep)	Molinelli waterfall, Forno valley, 1962 m.
D-158	PL, HBL, op, (chl), (cc)	Rio Ciose, southern side of the Forno valley, 2300 m.
D-109	PL, HBL, (BI.),qtz, ap, op, (chl), (ep), (ti), (cc), (wm)	High Pisella valley, over the Pisella lake, 2875 m.
D-189	HBL, PL, (BI),(QTZ), ap,op, zr, (chl), (ep), (ti), (ru)	Spur SSW of the Cedec Pass, Gran Zebrù, 3030 m.
D-55	PL, HBL, (GT),qtz, op, ap, (chl), (ti), (cc), (ep), (wm), (*)	Spur between the eastern and western Cedec glaciers, 3248 m.
D-196	HBL, PL, op, (ep), (cc), (chl), (ti), (**)	Spur SSW of the Cedec Pass, 3030 m.
D-28	PL, HBL, BI, cpx, qtz, op, (chl), (ep), (**)	Eastern wall of the peak 3293 m, south of Pale Rosse, 2950 m.
D-238	PL, HBL, (QTZ), (BI), op,(**)	Base of Punta Graglia, eastern Cedec glacier, 3050 m.
P-194	PL, HBL,(QTZ),(BI),op, ap, (chl), (wm)	Spur SSW of the Cedec Pass, 3040 m.
P-195	PL, HBL, (QTZ),bi, opx, op, (chl), (ti), (ep), (cc)	Idem
P-32	PL, HBL, BI,(QTZ),opx, cpx, ap, zr, (chl), (ep), (cc), (wm)	Eastern wall of the Pale Rosse-Peak 3293 ridge, 2976 m.
P-21	PL, HBL,(QTZ),kf, bi, op, (cc), (chl), (ti), (*), (**)	Front of the western Cedec glacier, 2950 m.
P-31	PL, HBL, (QTZ), (BI), cpx, ap, op, zr, (ep), (chl), (ti), (wm)	Eastern wall of the Pale Rosse-Peak 3293 ridge.
P-40	PL, HBL, (QTZ), (BI), op, ap, (chl), (ep), (ti), (wm)	Bottiglia Pass, SSW side, Gran Zebrù.
P-210	PL, HBL, (BI), (QTZ), op, (chl), (ti), (ep), (cc), (wm)	Bottiglia Pass, 3293 m.
P-20	PL, HBL, QTZ, BI, op, ap, zr, (chl), (ti), (ep), (cc)	Front of the western Cedec glacier, 2950 m.
P-38	PL, QTZ, BI, hbl, kf, ap, zr, op, (chl), (ti), (wm), (ep), (cc)	Bottiglia Pass, SSW side.
HIGH-K CALC-ALKALINE/SHOSHONITIC GROUP		
D-239	PL, HBL, (CPX), qtz, ap, op, (chl), (ep),(cc)	Middle Gavia valley/Alpe valley.
D-244	PL, HBL, (BI), qtz, op, (chl), (cc)	Idem
D-605	HBL, PL, (BI), op, ap, zr	Pala della Donzella, eastern side, 2570 m.
P-582	PL, HBL, BI, (QTZ), (KF), cpx, op, ap, (chl)	North of Malga Prabon, road to Malga Mare, 1825-1850 m.
P-602	PL, HBL, (CPX), (BI), (KF), (QTZ), op, ap, (chl), (ti)	Tof di Malè, eastern wall, 2530 m.
P-597A	PL, CPX, (HBL), (KF), (BI), (QTZ), op, ap, zr	Pala della Donzella, eastern wall, 2530 m.

P-581	PL, HBL, (BI), (QTZ), (KF), (CPX), op, ap, zr, (chl), (ti)	North of Malga Prabon, 1825-1850 m.
P-593	HBL, PL, (BI), (QTZ), (KF), op, ap, zr, (chl), (ti), (ep), (wm)	Tof di Malè, eastern wall, 2570 m.
M-592	HBL, PL, (BI), (CPX), qtz, kf, op, ap, (chl), (ti)	North of Malga Prabon, 1825-1850 m.
A-595	KF, PL, QTZ, (BI), op, ap, (ru)	Tof di Malè, eastern wall, 2510 m.
D-443	PL, HBL, bi, op, kf, zr, (wm), (chl), (ti)	Spur 3065-2832 m, 1 km NW of Grünsee, 2770 m.
D-417	HBL, BI, (PL), qtz, kf, op, ap, (chl)	Idem
P-440	PL, HBL, BI, (KF), (QTZ), ap, zr, (ep), (chl), (ti), (wm)	Idem, NE side, 2750 m.
P-454	PL, HBL, BI, (QTZ), op, ap, (chl), (ep)	500 m NW of Grünsee, 2650 m.
P-438	PL, HBL, BI, (QTZ), kf, ap, (chl), (ep), (cc)	Spur 3065-2832 m, 1 km NW of Grünsee, 2770 m.
P-422	PL, BI, HBL, QTZ, kf, cpx, op, ap, (ep), (wm), (chl), (ti)	Idem
M-453	PL, BI, HBL, qtz, op, ap, zr, (chl), (ti), (ep), (wm)	500 m NW of Grünsee, 2650 m.
A-446	KF, QTZ, (PL), (BI), ap, zr, (wm), (chl), (ru), (ti)	Spur 3065-2832 m, 1 km NW of Grünsee, 2570 m.
A-439	KF, QTZ, PL, bi, (chl), (ru), (wm)	Idem, 2770 m.

Capital letter: main and (in bracket) subordinate magmatic phases. Small letter: minor to accessory minerals. Small letter in bracket: secondary phases. (*) = partially altered rock; (**) = sample containing very small xenoliths of basement rocks. Ap: apatite, bi: biotite; cc: carbonate; chl: chlorite; cpx: clinopyroxene; ep: epidote; gt: garnet; hbl: hornblende; kf: K-feldspar; op: opaque; opx: orthopyroxene; pl: plagioclase; qtz: quartz; ru: rutile; ti: titanite; wm: white mica; zr: zircon.

References

ANDREATTA, C.: La formazione gneissico-kinzigitica e le oliviniti di Val d'Ultimo (Alto Adige). – Mem. Mus. St. Nat. Venezia Trid., **5**, 87–245, Trento 1935.

ANDREATTA, C.: Sulle rocce eruttive del Gruppo Ortles-Cevedale. – Rend. Acc. Italia, cl. Sc. Fis., **3**, 289–304, Roma 1942.

ANDREATTA, C.: La „Linea di Peio" nel massicio dell'Ortles e le sue miloniti. – Acta Geol. Alpina, 1, 63 p., Bologna 1948.

ANDREATTA, C.: Foglio Monte Cevedale. – Carta Geologica delle Tre Venezie, Magistrato alle Acque Venezia (Min. LL.PP.), Firenze 1951.

ANDREATTA, C.: La Val di Peio e la catena Vioz-Cevedale. – Acta Geol. Alpina, **5**, 336 p., Bologna 1954.

ARGENTON, A.: Studio geologico della Valle dei Forni. – Unpubl. Thesis, Ist. Geol. Univ., Padova 1978.

ARGENTON, A., DAL PIAZ, G.V., MARTIN, S. & SCHIAVON, E.: Osservazioni preliminari sul versante occidentale della dorsale Gran Zebrù – Cevedale – Corno dei Tre Signori (Austroalpino superiore, Alpi Orientali). – Rend. Soc. Ital. Min. Petr., **36**, 65–89, Milano 1980.

BARGOSSI, G.M., LUCCHINI, F. & MORTEN, L.: Masserelle periadriatichi affioranti lungo la Linea Insubrica fra Malé (Val di Sole) e Rumo (Val di Non). Studio petrografico modale. – Min. Petr. Acta, **22**, 13–28, Bologna 1978.

BECCALUVA, L., GATTO, G.O., GREGNANIN, A., PICCIRILLO, E.M. & SCOLARI, A.: Geochemistry and petrology of dyke magmatism in the Alto Adige (Eastern Alps) and its geodynamic implications. – N. Jb. Geol. Paläont. Mh., **6**, 321–329, Stuttgart 1979.

BECCALUVA, L., BIGIOGGERO, B., CHIESA, S., COLOMBO, A., GATTO, G.O., GREGNANIN, A., MONTRASIO, A., PICCIRILLO, E.M. & TUNESI, A.: Post collisional orogenic dyke magmatism in the Alps. – Mem. Soc. Geol. Ital., **26**, 341–359, Roma 1985.

BELLIENI, G., PECCERILLO, A. & POLI, G.: The Vedrette di Ries (Rieserferner) plutonic complex: petrological and geochemical data bearing on its genesis. – Contrib. Miner. Petr. **78**, 145–156, Heidelberg 1981.

BÖGHEL, H.: Zur Literatur über die „Periadriatische Naht". – Verh. Geol. B.-A., 163–169, Wien 1975.

BRACK, P.: Structures in the southwestern border of the Adamello Intrusion (Alpi Bresciane, Italy). – Schweiz. Miner. Petr. Mitt., **61**, 37–50, Zürich 1981.

CALLEGARI, E.: Geological and Petrological aspects of the magmatic activity at Adamello (Northern Italy). – Mem. Soc. Geol. Ital., **26**, 83–103, Roma 1985.

CERONI, G.: Studio geologico del versante sinistro dell'Alta Valle della Mare. – Unpubl. Thesis, Ist. Geol. Univ., Padova 1982.

CORNELIUS, H.P.: Die Herkunft der Magmen nach STILLE vom Standpunkt der Alpengeologie. – Sitzber. Österr. Akad. Wiss., math.-naturwiss. Kl., **158**, 543–570, Wien 1949.

DAL PIAZ, G.: Il confine Alpino-Dinarico dall'Adamello al Massiccio di Monte Croce nell'Alto Adige. – Atti Acc. Sc. Ven.-Trent.-Istriana, **17**, 3–7, Padova 1926.

DAL PIAZ, Gb.: Studi geologici sull'Alto Adige orientale e regioni limitrofe. – Mem. Ist. Geol. Univ. Padova, **10**, 1–245, Padova 1934.

DAL PIAZ, Gb.: La struttura geologica delle Austridi. Nota III. Il sistema austroalpino nelle Alpi Breonie e Venoste e nel massiccio dell'Ortles. Nuovo schema tettonico delle Austridi della Venezia tridentina e del Tirolo orientale. – Atti Rend. Acc. Sc. Torino, **71**, 1–29, Torino 1936.

DAL PIAZ, Gb.: Geologia della bassa Val d'Ultimo e del massiccio granitico di Monte Croce. – Mem. Museo St. Nat. Venezia Trid., **5**, 184 p., Trento 1942.

DAL PIAZ, G.V.: Alcune riflessioni sulla evoluzione geodinamica alpina delle Alpi. – Rend. Soc. Ital. Miner. Petr., **32**, 380–385, Roma 1976.

DAL PIAZ, G.V. (Ed.): Il magmatismo tardo alpino nelle Alpi. – Atti Convegno Padova 1983, Mem. Soc. Geol. Ital., **26**, 436 p., Roma 1985.

DAL PIAZ, G.V., HUNZIKER, J.C. & MARTINOTTI, G.: La Zona Sesia-Lanzo e l'evoluzione tettonico metamorfica delle Alpi nordoccidentali interne. – Mem. Soc. Geol. Ital., **11**, 433–466, Roma 1972.

DAL PIAZ, G.V. & LOMBARDO, B.: Review of radiometric dating in the Western Italian Alps. – Rend. Soc. Ital. Miner. Petr., **40**, 125–138, Milano 1985.

DAL PIAZ, G.V. & MARTIN, S.: I porfiroidi nelle filladi della Valle dei Forni, Falda dell'Ortles, Austroalpino superiore. – Rend. Soc. Geol. Ital., **3**, 17–20, Roma 1980.

DAL PIAZ, G.V. & VENTURELLI, G.: Brevi riflessioni sul magmatismo post-ofiolitico nel quadro della evoluzione spaziotemporale delle Alpi. – Mem. Soc. Geol. Ital., **26**, 5–19, Roma 1985.

DAL PIAZ, G.V., VENTURELLI, G. & SCOLARI, A.: Calc-alkaline to ultrapotassic postcollisional volcanic activity in the internal Northwestern Alps. – Mem. Sci. Geol., **32**, 1–16, Padova 1979.

DEL MORO, A., DAL PIAZ, G.V., MARTIN, S. & VENTURELLI, G.: Dati radiometrici e geochimici preliminari su magmatiti oligoceniche del settore meridionale del Massiccio Ortles-Cevedale. – Rend. Soc. Geol. Ital., **4**, 265–266, Roma 1981.

DEL MORO, A., PARDINI, G., QUERCIOLI, C., VILLA, I.M. & CALLEGARI, E.: Rb/Sr und K/Ar chronology of Adamello granitoids, Southern Alps. – Mem. Soc. Geol. Ital., **26**, 285–299, Roma 1985.

DEUTSCH, A.: Young Alpine dykes south of the Tauern Window (Austria): a K/Ar and Sr isotope study. – Contr. Miner. Petr., **85**, 45–57, Heidelberg 1984.

EXNER, Ch.: Die geologische Position der Magmatite des Periadriatischen Lineaments. – Verh. Geol. B.-A., **1976**, 3–64, Wien 1976.

FERRETTI TORRICELLI, F.: Studio geologico del versante destro dell'alta Valle della Mare. – Unpubl. Thesis, Ist. Geol. Univ., Padova 1982.

FREY, M., HUNZIKER, J.C., FRANK, W., BOCQUET, J., DAL PIAZ, G.V., JAEGER, E. & NIGGLI, E.: Alpine metamorphism of the Alps: a reviw. – Schweiz. Miner. Petr. Mitt., **54**, 247–290, Zürich 1974.

GANSSER, A.: The Insubric Line, a major geotectonic problem. – Schweiz. Miner. Petr. Mitt., **48**, 123–143, Zürich 1968.

GATTO, G.O., GREGNANIN, A., PICCIRILLO, E.M. & SCOLARI, A.: The andesitic magmatism in the South-Western Tyrol and its geodynamic significance. – Geol. Rdsch., **65**, 691–700, Stuttgart 1976.

GATTO, G.O., GREGNANIN, A., MOLIN, G.M., PICCIRILLO, E.M. & SCOLARI, A.: Le manifestazione andesitiche polifasiche dell'Alto Adige occidentale nel quadro geodinamico alpino. – Studi Trentini Sc. Nat., **53**, 21–47, Trento 1976.

GATTO, G.O. & SCOLARI, A.: La tettonica tardiva del ciclo orogenetico alpino nell'Alto Adige occidentale e regioni limitrofe. – Boll. Soc. Geol. Ital., **93**, 1211–1231, Roma 1974.

GREGNANIN, A., & PICCIRILLO, E.M.: Litostratigrafia, tettonica e petrologia degli scisti austridici di alta e bassa pressione dell'area Passiria – Venosta (Alto Adige). – Mem. Is. Geol. Miner. Univ. Padova, **28**, 55. p., Padova 1972.

GREGNANIN, A., & PICCIRILLO, E.M.: Hercynian metamorphism in the Austridic crystalline basement of the Passiria and Venosta Alps. – Mem. Soc. Geol Ital., **13** (suppl. 1), 241–255, Roma 1974.

GULSON, B.L.: Age relations in the Bergell region of the South-East Swiss Alps: with some geochemical comparisons. – Eclogae Geol. Helv., **66**, 293–313, Basel 1973.

HAMMER, W.: Die Ortlergruppe und der Ciavalatschkamm. – Jb. Geol. R.-A., **58**, 79–196, Wien 1908.

HAMMER, W.: Geologische Spezialkarte, Blatt Bormio und Passo del Tonale, und Erläuterung. – Wien (Geol. R.-A.) 1908.

HERZBERG, C., RICCIO, C., CHIESA, S., FORNONI, A., GATTO, G.O., GREGNANIN, A., PICCIRILLO, E.M. & SCOLARI, A.: Petrogenetic evolution of a spinel-garnet-lherzolite in the Austridic Crystalline Basement from Val Clapa (Alto Adige, Northeastern Italy). – Mem. Ist. Geol. Miner. Univ. Padova, **30**, 29 p., Padova 1977.

HUNZIKER, J.C. & MARTINOTTI, G.: Geochronology and evolution of the Western Alps: a review. – Mem. Soc. Geol. Ital., **29**, 43–56, Roma 1987.

KAGAMI, H., ULMER, P., HANSMANN, W., OBERLI, F., DIETRICH, V. & STEIGER, R.H.: Rb-Sr isotopic characteristics of the southern Adamello intrusives: implications for crustal versus mantle origin. – Convegno „Magmatismo tardo alpino nelle Alpi", SGI-SIMP. Abstract, Padova 1983.

KLEBELSBERG, R.: Geologie von Tirol. – Berlin (Borntraeger) 1935.

LAUBSCHER, H.P.: The large-scale kinematics of the Western Alps and Northern Apennines and its palinspastic implications. – Amer. J. Sci., **271**, 193–226, New Haven 1971.

LAUBSCHER, H.P.: Evoluzione e struttura delle Alpi. – Le Scienze, **72**, 264–275, Milano 1974.

LAUBSCHER, H.P.: The late Alpine (Periadriatic) intrusions and the Insubric Line. – Mem. Soc. Geol. Ital., **26**, 21–30, Roma 1985.

LAUBSCHER, H.P. & BERNOULLI, D.: History and deformation of the Alps. – In: K. HSÜ (Ed.): Mountain Building Processes. – 169–180, London (Academic Press) 1982.

MARTIN, S.: Studio geologico della Valle di Cedec. – Unpubl. Thesis, Ist. Geol. Univ., Padova 1978.

MINGUZZI, C.: Ricerche petrografiche sopra alcuni lamprofiri, porfiriti e dioriti della Val d'Ultimo. – Studi Trentini Sc. Nat., **21**, 1–46, Trento 1940.

PAPIKE, J.J., CAMERON, K.L. & BALDWIN, K.: Amphiboles and pyroxenes: characterization of other than quadrilateral components and estimates of ferric iron from microprobe data. – Geol Soc. Amer., Abstr. Progr., **6**, 1053–1054, Boulder 1974.

PIRKL, H.R.: Die westlichen Zentralalpen. – In: R. OBERHAUSER (Wiss. Red.): Der geologische Aufbau Österreichs, 332–347, Wien 1980.

POZZI, R.: Schema tettonico dell'alta Valtellina da Livigno al Gruppo dell'Ortles. – Eclogae Geol. Helv., **58**, 21–38, Basel 1965.

SASSI, F.P., CAVAZZINI, G., VISONA, D. & DEL MORO, A.: Radiometric geochronology in the Eastern Alps: results and problems. – Rend. Soc. Ital. Miner. Petr., **40**, 187–224, Milano 1985.

SATIR, M.: Die Entwicklungsgeschichte der westlichen Hohen Tauern und der südlichen Ötztalmasse auf Grund radiometrischer Altersbestimmungen. – Mem. Ist. Geol. Min. Univ. Padova, **30**, 84 p., Padova 1975.

SCHREYER, W., MASSONE, H.J. & CHOPIN, C.: Continental crust subducted to depths near 100 km: Implications for magma and fluid genesis in collision zones. – In: B.O. MYSEN (Ed.): Magmatitic processes: Physicochemical Principles. – Geochem. Soc. Special Publ., **1**, 155–163, 1987.

STACHE, G. & JOHN, C.: Geologische und petrographische Beiträge zur Kenntnis der älteren Eruptiv- und Massengesteine der Mittel- und Ostalpen. II. Das Cevedale-Gebiet als Hauptdistrict älterere dioritischer Porphyrite (Paläoporphyrite). – Jb. Geol. R.-A., **29**, 317–404, Wien 1878.

TOMASI, L.: Studi petrografichi dei filoni e contatti del Passo della Bottiglia (Gruppo dell'Ortles). – Acta Geol. Alpina, **2**, 49 p., Bologna 1950.

TOMBA, A.M.: Studio petrografico sopra alcune porfiriti del versante sinistro della media Val d'Ultimo (Alto Adige). – Period. Miner., **16**, 215–226, Roma 1947.

THÖNI, M.: Degree and evolution of the Alpine Metamorphism in the Austroalpine Unit W of the Hohe Tauern in the light of the K/Ar and Rb/Sr age determinations on micas. – Jb. Geol. B.-A., **124**, 111–174, Wien 1981.

THÖNI, M.: The Rb/Sr thin slab geologic isochron method – an reliable geochronologic method for dating geologic events in polymetamorphic terrains? – Mem. Sci. Geol., **38**, 283–352, Padova 1986.

TROMMSDORFF, V. & NIEVERGELT, P.: The Bregaglia (Bergell) – Iorio Intrusion and its field relations. – Mem. Soc. Geol. Ital., **26**, 55–68, Roma 1985.

TRÜMPY, R.: The Timing of Orogenic Events in the Central Alps. – In: K.A. DE JONG & R. SCHOLTEN (Eds.): Gravity and Tectonics, 229–251, New York (Wiley & Sons) 1973.

ULMER, P., CALLEGARI, E. & SONDEREGGER, U.C.: Genesis of the mafic and ultramafic rocks and their genetical relations to the tonalitic-trondhjemitic granitoids of the southern part of the Adamello Batholith (Northern Italy). – Mem. Soc. Geol. Ital., **26**, 171–222, Roma 1985.

VENTURELLI, G., THORPE, R.S., DAL PIAZ, G.V., DEL MORO, A. & POTTS, P.J.: Petrogenesis of calc-alkaline shoshonitic and associated ultrapotassic Oligocene volcanic rocks from the Northwestern Alps, Italy. – Contr. Miner. Petr., **86**, 209–220, Heidelberg 1984.

ZANETTIN LORENZONI, E.: Le porfiriti quarzodioritiche (telliti) di Tell, presso Merano (Alto Adige). – Atti Ist. Veneto Sci. Lett. Arti, C. m.-n., **122**, 229–292, Venezia 1964.

Manuskript bei der Schriftleitung eingelangt am 19. August 1988.